Experimental and Computational Study on the Properties of Pure and Water Mixed 1-Ethyl-3-methylimidazolium L-(+)-Lactate Ionic Liquid

Santiago Aparicio,*,† Rafael Alcalde,† and Mert Atilhan‡

Department of Chemistry, University of Burgos, 09001 Burgos, Spain, and Chemical Engineering Department, Qatar University, Doha, Qatar

Received: December 4, 2009; Revised Manuscript Received: March 12, 2010

Ionic liquids have attracted great attention, from both industry and academe, as alternative fluids for a large collection of applications. Although the term *green* is used frequently to describe ionic liquids in general, it is obvious that it cannot be applied to the huge quantity of possible ionic liquids, and thus, those with adequate environmental and technological profiles must be selected for further and deeper studies, from both basic science and applied approaches. In this work, 1-ethyl-3-methylimidazolium L-(+)-lactate ionic liquid is studied, because of its remarkable properties, through a wide-ranging approach considering thermophysical, spectroscopic, and computational tools, to gain a deeper insight into its complex liquid structure, both pure and mixed with water, thus implying the main factors that would control the technological applications that could be designed using this fluid. The reported results shows a strongly structured pure ionic liquid, in which hydrogen bonding, because of the hydroxyl group of the lactate anion, develops a remarkable role, together with Coulombic forces to determine the fluid's behavior. Upon mixing with water, the ionic liquid retains its structure up to very high dilution levels, with the effect of the ionic liquid on the water structure being very large, even for very low ionic liquid mole fractions. Thus, in water solution, the studied ionic liquid evolves from noninteracting ions solvated by water molecules toward large interacting structures with increasing ionic liquid content.

1. Introduction

Ionic liquids are attracting a great attention, both from industry and from academia, because of their promising properties in very different fields, ranging from basic science to applied purposes.[1] An analysis of the literature from the middle of the 1990s shows how these fluids have evolved from curiosities to compounds for which even a completely new chemistry may be thought.[2] These fluids are commonly, and uncritically, termed as *green*, and thus are included within the green chemistry framework, in contrast to the ubiquitous volatile organic compounds used for many applications including solvents. Frequently, their supposed *green* character is considered the main advantage of ionic liquids over traditional organic fluids, and thus, ionic liquid and *green* terms are usually considered as almost synonymous words. Nevertheless, the reported toxicological and biodegradability studies of some ionic liquids have showed that some of these fluids are not so *green* as initially supossed.[3] This fact should not be a problem if we consider that the number of theoretically possible ionic liquids is almost unlimited. This characteristic of ionic liquids, the possibility of considering them as task-specific fluids,[4] should be the main strength of this new technology, and it could lead to a new approach for chemistry in which we would be able to find the most adequate fluid for the desired purposes, thus improving the whole production cycle according to the green chemistry paradigm.

Although the task-specific character of ionic liquids, rising from the huge number of possible cation/anion combinations,[5] is the most important factor for this technology, it is also its main weakness if we are not able to understand the molecular level factors that govern their liquid phase properties and structure, and to develop reliable and accurate structure−property relationships.[6] Therefore, basic studies on carefully selected ionic liquids must be carried out to infer the main molecular level features that govern their liquid structures and their relationships with macroscopic properties. To carry out these studies requires a lot of effort, in human, time, and economic resources, and thus it cannot be done for all possible cation/anion combinations. Hence, a judicious selection of ionic liquids must be done,[7] considering several factors: (i) ions must show low toxicity, both for humans and the environment, (ii) ions must be produced from available sources through simple and economically viable procedures leading to feasible large-scale productions that allow competition with traditional organic fluids, and (iii) ionic liquids should have adequate properties for engineering purposes, such as moderate viscosity.

To design environmentally friendly ionic liquids, two very useful concepts, from the pharmaceutical and food industries, may be considered:[8] (i) nontoxic pharmaceutically acceptable ions and (ii) generally regarded as safe materials (GRAS). The list of ions included in these categories is large,[9] and thus it is not a strongly restrictive criterion that would hinder ionic liquids' technology development, with many of these ions leading to the formation of room temperature ionic liquids. The economically feasible production at a multiton scale of ionic liquids is a very important issue,[10] because the actual pricing of many of these fluids hinders the replacement of traditional fluids in large-scale plants. Although several large-scale industrial applications have been designed using ionic liquids,[11] it should be recognized that their use in the chemical and related industries is still rare. The reluctant position of industry to replace traditional fluids by ionic liquids rises from (i) the pricing of available ionic

* Corresponding author. E-mail: sapar@ubu.es.
† University of Burgos.
‡ Qatar University.

10.1021/jp911536z
Published on Web 04/09/2010

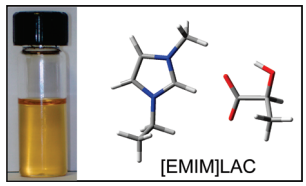

Figure 1. Liquid [EMIM]LAC at ambient conditions and molecular structure of the ionic pair calculated at B3LYP/6-311++g** theoretical level.

liquids, which is strongly related to their small-scale production, and (ii) the poor knowledge of the main properties of many of them. These problems could be solved if the ions pertaining to the GRAS and nontoxic pharmaceutically acceptable categories are considered as suitable candidates for ionic liquids production because many of them may be produced at large scale from easily available sources through simple and economically viable procedures. Moreover, these ions have been used for decades in the industry, and thus expertise has been developed that could be used for the development of ionic liquid technologies. These facts should guide in our opinion the research on ionic liquids, which should be carried out in a systematic way.

Thus, in this work we report a study on the properties of 1-ethyl-3-methylimidazolium L-(+)-lactate ionic Liquid, [EMIM]-LAC, pure and water mixed, using a wide collection of experimental and computational tools, that would allow inferring valuable information on its molecular level structure and its relationship with its macroscopic properties. This study is a continuation of previously reported ones,[12] in which the same approach was applied for carefully selected ionic liquids. Lactate anions are included in the nontoxic pharmaceutically acceptable and GRAS ions category,[9] and thus they show very good environmental and toxicological profiles. Lactate anions may be combined with alkyl imidazolium cations leading to ionic liquids through one-stage synthesis without byproduct, and using simple and cheap reactants such as lactic acid.[13] Moreover, organic solvents of the lactate family, such as ethyl lactate,[14] have been used in industry for decades for several applications. 1-Alkyl-3-methylimidazolium cations are known to have a certain toxicity and not very good biodegradability;[3] nevertheless, the environmental and toxicological profiles are remarkably better as the alkyl chain length decreases,[3] although this alkyl chain effect is controversial for benthic ecosystems,[15] and this is the motive to select 1-ethyl-3-methylimidazolium cation for this work. Moreover, 1-alkyl-3-methylimidazolium lactate ionic liquids undergo very effective decomposition through ozonation,[16] which would allow end-of-process treatment without risk for the environment.[16,17] The reported study uses a combination of several tools to get a deep insight into the studied fluid behavior. Spectroscopic results, using dielectric relaxation spectroscopy (DRS), attenuated total reflectance infrared spectroscopy (ATR-FTIR), and solvatochromic studies, are reported together with relevant thermophysical properties (density, speed of sound, refractive index, viscosity, and isobaric heat capacity) and computational studies according to density functional theory and molecular dynamics approach. [EMIM]LAC is studied in the pure state and also as water mixed, to understand the effect of water cosolvent on ionic liquid structure and the effect of the ionic liquid on the water hydrogen bonding network.[18]

2. Materials and Methods

2.1. Materials. [EMIM]LAC (CAS Registry Number 878132-19-5) was obtained from Aldrich; it is a viscous and light brownish-yellow liquid, as shown in Figure 1. The color of ionic liquids is considered as an indicator of impurities, and thus several synthetic procedures have been proposed to obtain ultrapure transparent ionic liquids.[19] Nevertheless, the origin of the color of ionic liquids is still not fully understood. It has been proposed that it may be originated by overheating in synthetic procedures, but it may be also produced by the presence of chromophoric species of different natures rising from side reactions.[19b] Moreover, it should be noted that even a colorless ionic liquid is not necessarily pure,[20] and in general, the impurities leading to the color of ionic liquids are usually present at very low concentration; thus their effect on most of the ionic liquid properties is almost negligible and their removal would be necessary only for very specific applications such as for certain catalytic purposes.[1b,19,21] Therefore, removal of [EMIM]LAC color was not tried and the colored sample was used in this work. Nevertheless, it is important to analyze and report these impurity concentrations to obtain reproducible results. Thus, [EMIM]LAC samples were heated under vacuum for 72 h before use and kept under inert atmosphere. Water content was measured through Karl Fischer coulometric titration; the water content for all samples was lower than 500 ppm. Halide contents measured through ion chromatography were 30 ppm for Br^- and 49 ppm for Cl^-. Other relevant ions measured through the same technique were NO_3^- (10 ppm), PO_4^{3-} (57 ppm), and SO_4^{2-} (15 ppm). The purity of [EMIM]LAC, measured through HPLC relative areas, was always better than 99%.

Ultrapure water (Milli-Q, Millipore, 18.2 mΩ·cm resistivity) was used for all experiments. Mixture samples were prepared by weighing with a Mettler AT261 balance ($\pm 1 \times 10^{-5}$ g), thus leading to $\pm 1 \times 10^{-4}$ accuracy for mole fraction.

2.2. Ambient Pressure Thermophysical Properties. Density (ρ) and speed of sound (u) were measured simultaneously with an Anton Paar DSA 5000 instrument, where density was measured by an oscillating U-tube ($\pm 5 \times 10^{-6}$ g cm^{-3}) and the speed of sound was determined by measuring the traveling time of a sound pulse from the piezoelectric transducer to the detector (± 0.5 m s^{-1}). The cell temperature was controlled by a built-in solid-state thermostat and measured by internal platinum resistance thermometers ($\pm 1 \times 10^{-2}$ K). Calibration was carried out using two reference standards, *n*-nonane (Fluka, purity >99.5%) and toluene (Sigma-Aldrich, purity >99.5%). Density values for these standards were obtained from the literature.[22]

Dynamic viscosity (η) was measured using an automated AMV200 Anton Paar rolling ball microviscometer. The cell temperature was controlled through a Julabo F25 external thermostat and measured with a platinum resistance thermometer ($\pm 1 \times 10^{-2}$ K). The rolling time was measured to $\pm 1 \times 10^{-2}$ s, then precision for dynamic viscosity was $\pm 5 \times 10^{-3}$ mPa s. Calibration was carried out using *n*-dodecane (Aldrich, >99.5%), hexan-1-ol (Fluka, >99.5%), octan-1-ol (Fluka, >99.5%), decan-1-ol (Fluka, >99.5%) and ethylenglycol (Fluka, > 99.5%) as standards.[22,23]

Refractive indices (n_D) were measured in relation to the sodium D line by an automated Leica AR600 refractometer to $\pm 5 \times 10^{-6}$. Temperature was controlled by a Julabo F32 external circulator and measured by a platinum resistance thermometer ($\pm 1 \times 10^{-2}$ K). Calibration was performed using double degassed water (Millipore Milli-Q) and a standard oil ($n_D = 1.514\,16$) supplied by the manufacturer.

Isobaric molar heat capacities (C_p) were measured to $\pm 1 \times 10^{-2}$ J mol^{-1} K^{-1} using a Setaram micro DSC III calorimeter. It consists of two vessels (reference and measuring) surrounded by an array of highly sensitive Peltier elements ($\pm 1 \times 10^{-2}$ K),

and lodged in a calorimetric block surrounded by a thermostatic liquid (*n*-undecane) that ensures a temperature homogeneity. The calorimeter works under the Calvet principle, determining the variation of the heat flow to/from the liquid, with both cells maintained at the same temperature. Measurements were performed according to the isothermal step method described in the literature,[24] using *n*-hexane (Fluka, >99.5%) as reference material and butan-1-ol (Aldrich, >99.5%) as calibration liquid, whose C_p values were obtained from Zabransky et al.[25]

Excess properties derived from experimental ones were calculated according to well-known ideality criteria.[26,27] If an ideal term may not be defined, as for viscosity or refractive index, and thus it is not proper to use the term *excess*, the so-called mixing property according to eq 1 is used.

$$\Delta Y = Y - \sum_{i=1}^{2} x_i Y_i \quad (1)$$

Conductivity measurements (±1%) were carried out using a Radiometer CDM210 conductivity meter, previously calibrated using KCl standard solutions. Electrode and samples were placed in a sealed glass cell, immersed in a Julabo F32 bath. The sample temperature (±0.01 K) was measured with a platinum resistance thermometer.

2.3. Spectroscopic Measurements. UV−vis measurements were performed in a Hewlett-Packard spectrophotometer (±0.2 nm) with the temperature of the cell controlled with a Peltier element to $\pm 1 \times 10^{-1}$ K. Reichardt's dye (Aldrich 95%) was used for solvatochromic measurements according to a procedure previously reported.[28] Attenuated total reflection infrared (ATR-FTIR) spectroscopy studies were developed with a Nicolet Nexus spectrometer together with a Smart Thermal ARK device. The ATR accessory contains a zinc selenide crystal, the temperature of which is controlled through a built-in controller, and measured through an RTD temperature sensor to ±1 °C. Microwave dielectric relaxation spectroscopy (DRS) measurements were performed according to a coaxial reflection technique using a vector network analyzer (Agilent N5230A) in the 200 MHz−20 GHz frequency range with an Agilent 85070E dielectric probe kit and an Agilent N4691B ECal electronic calibration module. The cell temperature was controlled with an external circulating bath and measured to $\pm 1 \times 10^{-1}$ K with a platinum resistance thermometer; the measurement and calibration procedures were previously reported.[29]

2.4. Density Functional Theory (DFT) Calculations. DFT calculations were carried out with the Gaussian 03 package[30] according to density functional theory, using the Becke gradient corrected exchange functional[31] and the Lee−Yang−Parr correlation functional[32] with three parameters (B3LYP)[33] method. The 6-311++g** basis set was used in this work. Atomic charges were calculated to fit the electrostatic potential[34] according to the Merz−Singh−Kollman (MK)[35] scheme. Interaction energies for complexes, ΔE, were calculated as the differences among the complex and sum of monomers' energies at the same theoretical level, with basis set superposition error (BSSE) corrected through the counterpoise procedure.[36]

2.5. Classical Molecular Dynamics (MD) Simulations. Classical molecular dynamics simulations were carried out using the TINKER molecular modeling package.[37] All simulations were performed in the NPT ensemble; the Nosé−Hoover method[38] was used to control the temperature and pressure of the simulation system. The motion equations were solved using the Verlet Leapfrog integration algorithm.[39] The molecular geometries were restrained according to the shake algorithm.[40] Long-range electrostatic interactions were treated with the smooth particle mesh Ewald method.[41] The simulated systems consist of cubic boxes with 150 ionic pairs for pure [EMIM]-LAC, and of different ratios of water/[EMIM]LAC molecules (see Results) for mixtures, to which periodic boundary conditions were applied in three directions. The simulations were performed using a cutoff $L/2$ Å radius for the nonbonded interactions, with L being the box side. Initial boxes were generated using the PACKMOL program[42] that uses the BOX-QUACAN[43] local-minimization method to obtain adequate starting configurations. These boxes were minimized according to the MINIMIZE program in TINKER package to a 0.01 kcal mol^{-1} $Å^{-1}$ *root-mean-square* gradient. Then, several heating and quenching steps in the NVT ensemble up to 500 K were performed, after which 200 ps NVT equilibration molecular dynamics simulations were run at the set temperature; finally, from the output NVT simulation configurations, runs of 5 ns (time step 1 fs) in the NPT ensemble at the set temperatures and 0.1 MPa were run, from which the first 2 ns was used to ensure equilibration (checked through constant energy) and the remaining 3 ns was used for analysis. Although [EMIM]LAC and its mixtures with water for low water levels have low self-diffusion coefficients (2 orders of magnitude lower than common organic solvents; see Results), the simulation time is large enough to obtain representative results of fluid properties and structures. [EMIM]LAC was described according to the so-called optimized potential for liquid simulations (*all-atom* version) OPLS-AA.[44] MK charges obtained through B3LYP/6-311++g** calculations were used in the simulations. Force-field parametrization is explained under Results. The SPC-E model was used for water molecules.[45]

3. Results

3.1. Pure [EMIM]LAC. ***3.1.1. Spectroscopic Measurements.*** The spectroscopic study was performed using three techniques: (i) microwave DRS, (ii) ATR-FTIR, and (iii) UV−vis solvatochromic studies using Reichardt's dye. One of the main concerns in the properties of an ionic liquid is its polarity. There has been remarkable controversy between the different sets of dielectric constants obtained through different approaches.[46−49] To characterize the polarity of [EMIM]LAC, we have used different approaches: the first and obvious choice is to carry out DRS measurements that should provide direct measurements of the dielectric constant; nevertheless, the highly electrical conductive character of ionic liquids leads to short-circuit measurements in which the relaxation signal is hidden by the conductivity contribution and the zero-frequency extrapolation of the real part of the dielectric spectra, which should lead to values of the static dielectric constant, is not simple. Nevertheless, this method has been applied with success for different ionic liquids,[46,50−52] and thus microwave DRS, in the 200 MHz−20 GHz frequency range, was applied in this work to (i) obtain the dielectric constant as a function of temperature and (ii) characterize the relaxational behavior of [EMIM]LAC. The total complex dielectric response, $\eta^*(\nu)$, is the quantity measured, which is related to the complex dielectric function, $\varepsilon^*(\nu)$, and the conductivity contribution that should be subtracted to obtain dielectric values:

$$\eta^*(\nu) = \varepsilon^*(\nu) - \mathrm{i}\frac{\sigma}{2\pi\nu\varepsilon_0} = \varepsilon'(\nu) - \mathrm{i}\left(\varepsilon''(\nu) + \frac{\sigma}{2\pi\nu\varepsilon_0}\right) \quad (2)$$

where ε' stands for the frequency-dependent permittivity and ε'' stands for the dielectric loss. The conductivity parameter, σ, is treated as a fitting parameter in the data numeric treatment. For [EMIM]LAC the analysis of experimental dielectric results was done successfully according to a relaxation time distribution involving two Debye processes:

$$\varepsilon^*(\nu) = \sum_{i=1}^{k} \frac{\Delta\varepsilon_i}{1 + 2i\pi\nu\tau_i} + \varepsilon_\infty \qquad (3)$$

where i stands for the imaginary unit, ν stands for the frequency, ε_∞ stands for the dielectric constant in the high-frequency limit, $\Delta\varepsilon_i$ stands for the relaxation amplitude of the i process, and τ_i stands for the relaxation time. The parameters were obtained by a least-squares procedure. The static permittivity or dielectric constant, ε_s, is also obtained from the experimental results.

The conductivity of [EMIM]LAC as a function of temperature is measured, and these experimental values are initial guesses in the fitting procedure. The fitted dc conductivities are close to the experimental values; see Table S1 (Supporting Information). The high-frequency limit of our experiments, 20 GHz, does not allow obtaining reliable values of ε_∞, mainly for the higher temperatures, because processes at higher frequencies are lost, and thus the reported values of ε_∞ [Table S1 (Supporting Information)] should be considered as estimates including both ε_∞ ($\sim n_D^2$) and hidden processes at higher frequencies. Dielectric constant values as a function of temperature reported in Table S1 (Supporting Information) are physically reasonable, showing a moderately polar fluid in agreement with previously reported data for other ionic liquids.[46,50−52] It should be remarked that the obtained dielectric constant for [EMIM]LAC is close to the value of the related molecular fluid ethyl lactate:[53] at 298.15 K the values are 15.70 for ethyl lactate and 14.90 for [EMIM]LAC.

The analysis of microwave DRS spectra according to two Debye processes shows a slower and more intense process, process 1, and a faster and weaker process, process 2 [Table S1 (Supporting Information)]. The relaxation amplitudes of both processes decrease upon temperature increase and they also move to lower times and faster relaxations, as the temperature increases, as may be expected (Figure 2). Process 1, centered in the 0.6−2.7 GHz range, appears in this range for all imidazolium-based liquids,[51,52] and it has been ascribed to the reorientation of dipolar cations.[51,52,54] To confirm this assignment, DFT at B3LYP/6-311++g** theoretical level calculations on dipole moments of gas phase isolated $[EMIM]^+$ cation and LAC^- anion, relative to their center of mass, were performed [Figure S1 (Supporting Information)]. The dipole moment of LAC^- anion is remarkably larger than that for $[EMIM]^+$, and thus for this ionic liquid the process 1 relaxation cannot be assigned exclusively to the collective relaxation of cationic dipolar species and an anionic contribution should be also considered. The large dipole moment of LAC^- should lead to ion pairs that could contribute to the long-time component of the dielectric signal. Nevertheless, considering the relatively slow character of dielectric relaxation methods, only pairs with long lifetimes could be seen; for moderately polar fluids such as [EMIM]LAC, ionic pairs are presumed to be short-lived and thus their contribution to process 1 should be minor.[55] Thus, in our opinion, process 1 should be assigned to the collective relaxation of both independent cations and anions. The relaxation time of process 1 shows an Arrhenius-type behavior, (Figure 2c); with an activation energy of 15.4 kJ mol^{-1}, this value is typical of cooperative dipolar rearrangement in hydrogen bonded liquids.[50]

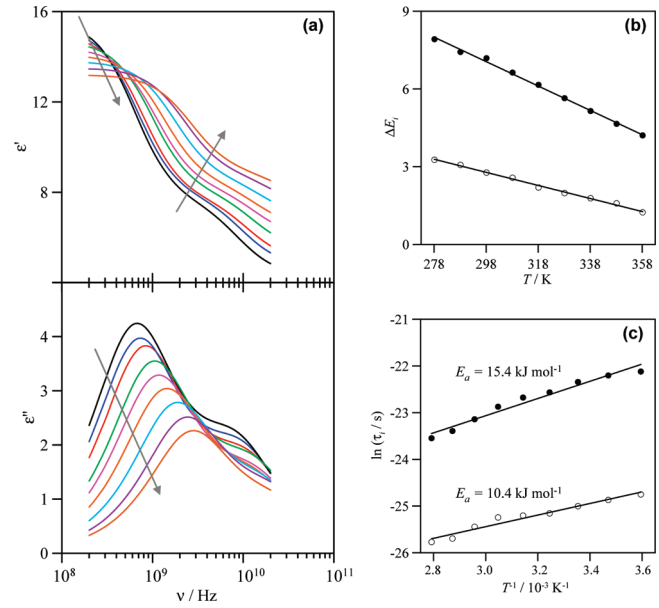

Figure 2. (a) Real, ε', and imaginary, ε'', parts of the complex dielectric function. (b) Relaxation amplitudes and (c) relaxation times, τ_i, obtained from the fit of experimental dielectric spectra according to two Debye processes, for pure [EMIM]LAC as a function of temperature, T. Solid lines in ε' and ε'' panels are obtained considering two Debye processes and parameters from Table S1 (Supporting Information); experimental points are not included for the sake of clarity. Panels b and c: processes (●) 1 and (○) 2; (—) lineal fittings for guiding purposes or to show Arrhenius-type behavior (panel c). In panel c, values of Arrhenius activation energy for relaxation times, E_a, are reported.

The origin of process 2 relaxation, centered in the 9−25 GHz frequency range, is not clear. Its amplitude is smaller than that for process 1, and it shows an activation energy lower than that for process 1 (Figure 2c). Recent studies have showed that it may be assigned to a cross-correlation of translational and rotational modes;[56] considering the large dipolar moment of the LAC^- anion and the moderate value for $[EMIM]^+$, both modes should contribute to process 2, although the rotational contribution should be larger and dominated by anion rotation because of its larger dipole moment.

Another frequent way to measure ionic liquid polarity is based on the behavior of different dyes dissolved in these fluids.[57] In this work, we have studied the solvatochromic behavior of Reichardt's betaine dye in [EMIM]LAC as a function of temperature, and the possible relationships between derived polarity parameters ($E_T(30)$ and E_T^N)[57] and the measured dielectric constant obtained through DRS measurements. Results of this study are reported in Table S2 (Supporting Information). Reichardt's parameters obtained in this work are very close to that for the molecular solvent ethyl lactate,[53] although the temperature effect on the parameters for [EMIM]LAC is very weak in comparison with the strong effect on ethyl lactate. If a linear relationship between $E_T(30)$ and the dielectric constant is considered,[48] a value of ~37 is inferred at 298.15 K for the dielectric constant of [EMIM]LAC. Although it may be argued that the error of the dielectric constant obtained from DRS measurements may be large, because of the conductivity contribution at low frequencies, it is obvious that the DRS value of ~15 is clearly different from the value inferred from solvatochromic measurements. Moreover, although the dipolar moment of the LAC^- anion would justify a larger dielectric constant than ionic liquids containing almost apolar anions, it is not large enough to justify such a large dielectric constant as that inferred from $E_T(30)$ measurements. If the dielectric constant

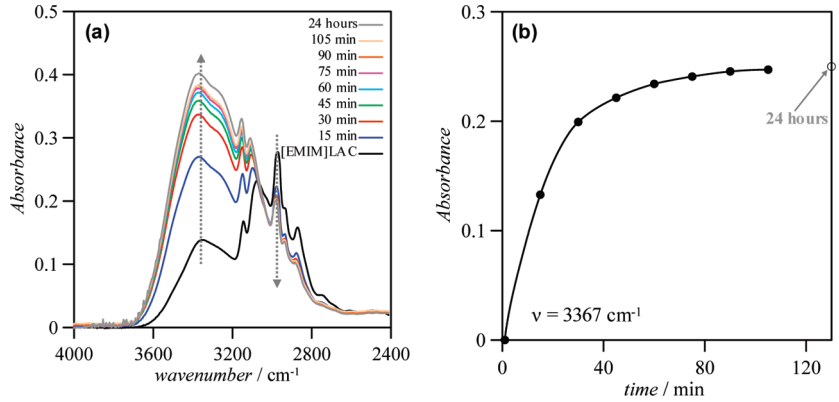

Figure 3. (a) ATR-FTIR spectra of [EMIM]LAC showing the water uptake at 298.15 K and (b) absorbance at 3367 cm^{-1} as a function of time exposure to atmospheric water. In panel b, data for pure [EMIM]LAC were subtracted. Atmospheric relative humidity ~50%.

of the related solvent ethyl lactate were inferred from its $E_T(30)$ values,[53] a very large value, also ~37, would be inferred in contrast with the experimental value of ~16 reported in the literature.[53,58] Thus, a direct and simple relationship between the dielectric constant, as a measure of ionic liquid polarity, and $E_T(30)$ parameters cannot be established.

Köddermann et al.[48] developed a method in which ATR-FTIR analysis of absorbed water vibrational modes in the OH stretching region lead to values of the dielectric constant. Thus, ATR-FTIR was used in this work for three main purposes: (i) to obtain dielectric constant values to compare with DRS ones, (ii) to study atmospheric water absorption in [EMIM]LAC, and (iii) to infer structural information. According to the Ködermann et al. procedure,[48] water solutions in [EMIM]LAC at 1 wt % (for this concentration water molecules are isolated from each other)[48] were prepared, and the positions of water symmetric, ν_1, and asymmetric, ν_3, OH-stretching bands, appearing in the 3000−3800 cm^{-1} range were analyzed through band deconvolution. This deconvolution is not simple for the [EMIM]LAC + 1 wt % water mixture because the OH-stretching band of LAC^- overlaps with ν_1 and ν_3 water bands; DFT gas-phase calculations show that the OH-stretching lactate peak appears at 3448 cm^{-1}. Pure [EMIM]LAC spectrum was subtracted from that of [EMIM]LAC + 1 wt % water mixture, and the resulting spectrum was deconvoluted [Figure S2 (Supporting Information)]. The ν_1 and ν_3 peaks appear at frequencies strongly red-shifted to the values in the water gas phase (185.1 and 196.3 cm^{-1}, respectively),[48] thus showing a strong interaction between water and [EMIM]LAC, mainly through the anion. Nevertheless, the application of the Ködermann et al. procedure[48] leads to a very large dielectric constant of ~37 in contrast to the DRS value of ~15. The values obtained by this method overestimate the ionic liquid dielectric constant; for example, Ködermann et al.[48] reports a value of ~15 for [EMIM]Tf_2N whereas the experimental value is 12.3[59] (22% larger) and for [EMIM]$EtSO_4$ (which contains an anion of remarkable polarity as in this case of LAC^-) a value of ~38 is reported (close to the value obtained for [EMIM]LAC) in contrast to the experimental value of 27.9 (36% larger)[59] or 35.20[60] (only 8% larger). Nevertheless, the dipole moment of the $EtSO_4^-$ anion is ~11.2−13.2 D (depending on its conformations),[60] which is 3 times larger than the value for the LAC^- anion, and thus the dielectric constant of [EMIM]LAC ionic liquid should be remarkably lower than the value for [EMIM]$EtSO_4$, with the values around 37 predicted by the Ködermann et al.[48] method for [EMIM]LAC being clearly too large. The possible reason for the large red-shifting of water ν_1 and ν_3 peaks compared with gas phase values[48] may be the presence of the OH group in LAC^- anion that leads to the development of strong hydrogen bonding between water molecules and this group.

ATR-FTIR was also used to study atmospheric water absorption. The effect of water on ionic liquid properties is well-known.[61] Hence, although ionic liquid samples may be prepared with reasonably low water contents, the hygroscopic character of many ionic liquids, such as [EMIM]LAC, would make it difficult, with moderate economic costs for multiton scales, to use absolutely dry ionic liquids for industrial purposes. Therefore, it is necessary to study water absorption to characterize their behavior toward moisture absorption. A sample, a small droplet, of previously dried [EMIM]LAC (500 ppm water content) was placed on the ATR-FTIR zinc selenide crystal, open to the atmosphere (~50% relative humidity), and the spectra were recorded for different times at 298.15 K (Figure 3).[62] The results show (i) saturation reached after around 2 h of atmospheric exposure and (ii) a very fast water uptake, with 50% of saturation water content after just 15 min of exposure. Thus, [EMIM]LAC must be handled with caution if water absorption is not desired, because a remarkably large water content may be obtained after short exposures to atmospheric moisture. Equilibrium concentration of water absorbed may be calculated from experimental ATR-FTIR absorbance data using molar absorptivity coefficients of water stretching bands obtained from measurements of water dissolved in CH_2Cl_2,[62] and effective path lengths can be determined according to Harrick's method,[62,63] using the Lambert−Beer law. Nevertheless, it should be remarked that for these calculations the molar absorptivity coefficients are supposed to be independent of the surrounding media (the same values for water bands in CH_2Cl_2 and [EMIM]LAC), which is obviously a simplification, and thus, in this work a different procedure has been used to measure water content. Different amounts of water were added to dried [EMIM]LAC and the ATR-FTIR spectra were measured,[64] and the absorbance at 3367 nm (wavelength for peak maxima, Figure 3a) was measured as a function of water molar concentration. Thus, using this procedure, the concentration of water in [EMIM]LAC in equilibrium with water from the atmosphere at 298.15 K is 30.77 mol dm^{-3}. This result shows the extremely hygroscopic character of [EMIM]LAC ionic liquid. Similar results have been reported in the literature for highly hygroscopic ionic liquids such as [EMIM]ethyl sulfate.[65] To confirm this water absorption behavior, gravimetric measurements were also performed.[65] A dried sample of [EMIM]LAC (2 g) was placed in a Petri disk, open to the atmosphere at ~293 K and 50% relative humidity, and without stirring, its weight was recorded ($\pm 1 \times 10^{-5}$ g) as a function of time [Figure S3 (Supporting Information)]. These gravimetric results confirm the extremely

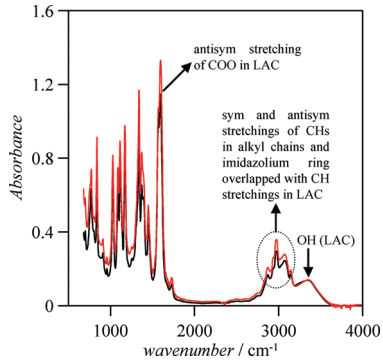

Figure 4. ATR-FTIR spectra of [EMIM]LAC at 298.15 K (black line) and 358.15 K (red line).

hygroscopic character of [EMIM]LAC; the absorption rate is lower for these gravimetric measurements in comparison with ATR-FTIR results reported in Figure 3 (around 2 h for saturation for ATR-FTIR in comparison with around 48 h for gravimetric experiments) because of the lower surface of sample exposed to the atmosphere used for gravimetric experiments.

ATR-FTIR measurements were also performed on dried [EMIM]LAC as a function of temperature to infer structural information on the studied ionic liquid. The spectra are reported in Figure 4 for the 500−4000 cm^{-1} range. The wide band with a maximum at 3360 cm^{-1} is assigned to the OH-stretching band in LAC^- anion; this band is red-shifted to the value calculated using DFT for the gas phase isolated anion (3448 cm^{-1}), and thus a stronger hydrogen bonding through this position is developed in comparison with the intramolecular hydrogen bonding in isolated gas phase anion. The group of bands in the 2700−3200 cm^{-1} region rises from the symmetric and antisymmetric CH bands of alkyl chains and CH groups in imidazolium rings overlapping with similar bands from CH groups in LAC^- cation. The peak for the stretching vibration of the C(2)-H group in the imidazolium ring, the acidic position through which the interaction with the anion for imidazolium containing ionic liquids is commonly developed, appears at 3072 cm^{-1}, which is 212 cm^{-1} red-shifted of the DFT value calculated for the isolated cation in the gas phase, and thus, interaction with the LAC^- anion through this position is confirmed. Finally, the peak at 1596 cm^{-1} is assigned to the antisymmetric vibration of the COO^- group in LAC^- anion; it is red-shifted 83 cm^{-1} of the DFT gas value of the anion because of the interaction with the cation.

3.1.2. Thermophysical Measurements. These properties are useful because (i) they are required for process design purposes and, thus, the absence of accurate data may hinder industrial application of ionic liquids, and (ii) they provide information on fluid structures. To our knowledge, no literature data are available for this fluid. The collection of thermophysical properties measured in this work, selected because of their industrial interest, are reported in Table S3 (Supporting Information). [EMIM]LAC is a moderately dense and remarkably viscous fluid. The viscous character of this ionic liquid confirms the existence of strong interactions between anions and cations which hinder the fluid flow. Moreover, this fluid has a large isobaric heat capacity that makes it suitable for heat transfer/thermal storage purposes. The calculated thermal storage density[12a] for a 100 °C differential is 201 MJ m^{-3}; this value is remarkably larger than the common heat transfer fluid requirements.[66] Moreover, the thermal storage density of [EMIM]LAC is larger than those for other ionic liquids with imidazolium cations but with anions with worse environmental profiles.[66]

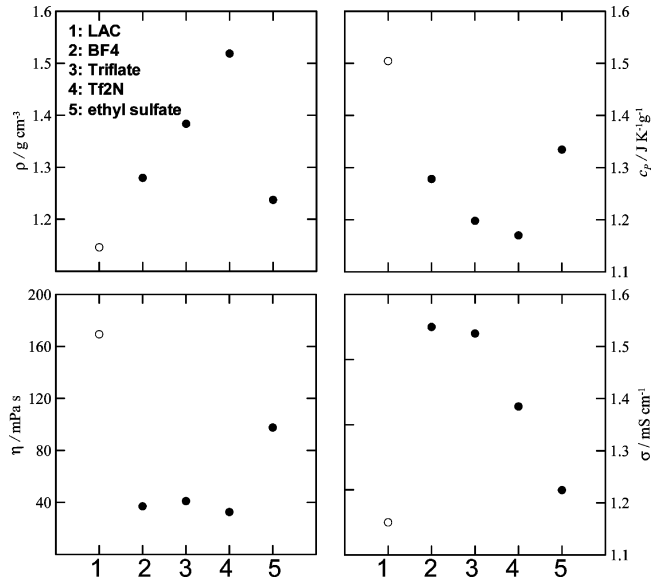

Figure 5. Comparison of selected experimental thermophysical properties at 298.15 K and 0.1 MPa for ionic liquids containing $[EMIM]^+$ cation with different anions. ρ, density, c_p, isobaric specific heat capacity, η, dynamic viscosity, and, σ, conductivity. Triflate, trifluoromethanesulfonate; Tf_2N, bis(trifluoromethylsulfonyl)imide. Data from ref 67.

Viscosity is another important property both to characterize ionic liquids and for industrial purposes. The viscous character of [EMIM]LAC may seem to hinder the use of this fluid for many applied purposes. To consider [EMIM]LAC as an alternative for heat transfer fluids, it should have a lower viscosity because in these applications fluids are used under flow conditions and, thus, viscosity may be a limiting factor if pumping costs become too large. Nevertheless, the viscosity of [EMIM]LAC decreases remarkably with temperature [Table S3 (Supporting Information)], and moreover, addition of other cosolvents, such as water, also decreases the viscosity, keeping the fluid performance.

The use of ionic liquids containing the LAC anion may have several advantages over other imidazolium-containing ionic liquids from the viewpoint of their thermophysical properties. To show the better profile of LAC-containing ionic liquids, several relevant thermophysical properties are reported for ionic liquids containing the $[EMIM]^+$ cation and different anions (Figure 5). The reported results show a certain proximity between LAC anion and the ethyl sulfate one (which also shows a good environmental profile). Thus, LAC ionic liquids show remarkably adequate thermophysical properties for industrial purposes in comparison with other imidazolium-containing ionic liquids. This fact, together with its better toxicological and environmental properties and its lower cost, makes it an alternative for common organic fluids clearly superior to other ionic liquids.

Finally, the structure of [EMIM]LAC may be analyzed considering the close relationship between conductivity and viscosity (Figure 6). Both conductivity and viscosity show non-Arrhenius behavior, and their temperature evolution may be described using a Vogel−Fulcher−Tamman (VFT) equation.[69,70] From the VFT parameters reported in Figure 6, the fragility parameter, F, defined according to Angell's criteria ($F = T_0/B$),[71] may be calculated. Thus, fragility parameters of 1.17 and 0.74 are obtained if viscosity and conductivity data are used, respectively, and thus this ionic liquid may be classified as a very fragile fluid, which will justify its large viscosity and low conductivity. The relationship between conductivity and viscos-

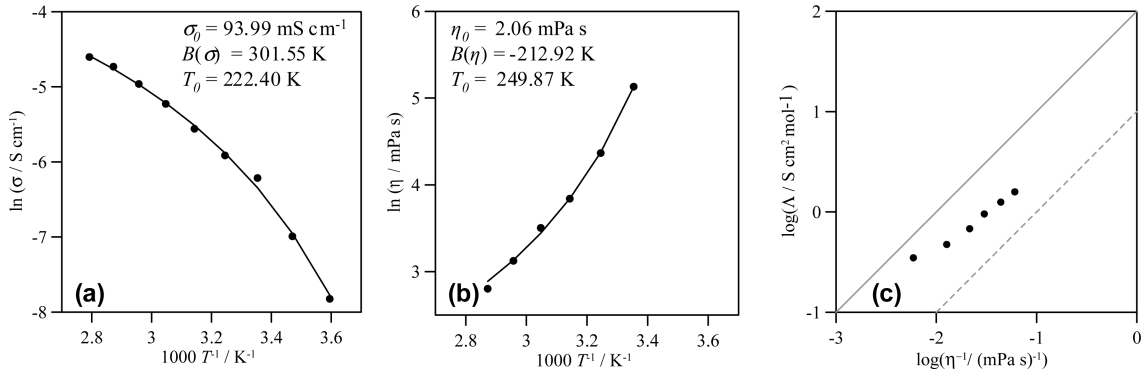

Figure 6. (a) Experimental conductivity, σ, (b) experimental dynamic viscosity, and (c) Walden plot for pure [EMIM]LAC as a function of temperature, T. Points show experimental data, and lines in panels a and b show VFT fits with fitted parameters reported within each panel. In panel c, the continuous line shows the ideal line according to ref 68 and the dashed line shows the situation of a liquid 10% ionized.

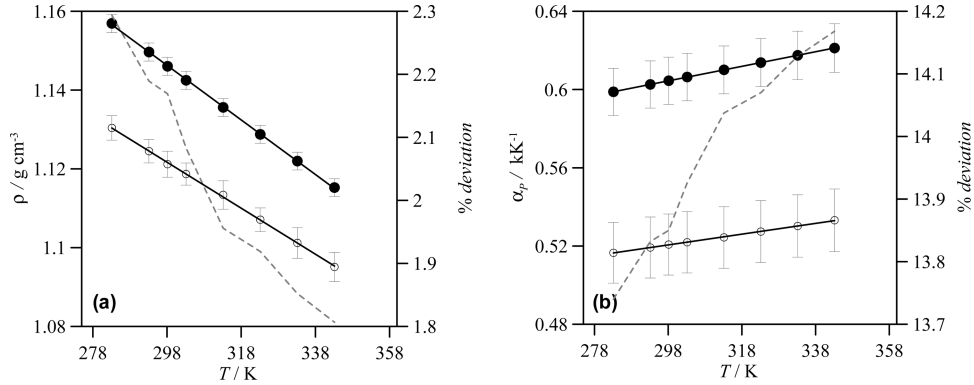

Figure 7. Experimental and calculated (molecular dynamics simulations with parameters reported in Table S4, Supporting Information) properties as a function of temperature at 0.1 MPa for [EMIM]LAC. Density, ρ, and isobaric thermal expansivity, α_P. Filled circles, experimental values; empty circles, molecular dynamics values; continuous lines, guiding lines; gray dashed lines, percentage deviations. α_P calculated from experimental density data using thermodynamic relations and from molecular dynamics simulations using fluctuation equations.

ity may be analyzed using Walden plots (Figure 6c), in which the molar conductivity log function is plotted vs the log of fluidity; this method has been applied previously to analyze the concept of ionicity in ionic liquids.[72] In this plot, values for [EMIM]LAC are compared with those for a 0.01 M KCl solution, the so-called ideal line, which allows the placement of a reference line. Literature values for ionic liquid usually fall below the ideal line (that shows the behavior of fully dissociated and equal mobility ions);[73] this is also true for [EMIM]LAC, and thus it may be classified as a subionic fluid,[74] showing the association between involved ions. To quantify the deviations from the ideal reference line, ΔW, defined as the vertical deviation from the ideal line, is calculated,[74] and thus values of 0.58 and 0.23 for 348.15 and 298.15 K are obtained, respectively, with a remarkable change on going from 308.15 K (ΔW = 0.43) to 298.15 K. The position of results for [EMIM]LAC, in the middle between the reference line and the line showing a liquid only 10% ionized, allows inferring a high ionicity for this ionic liquid.[74]

3.1.3. Molecular Dynamics Simulations. The results obtained through classical molecular dynamics simulations allow inferring more detailed information on structural and dynamic features at the molecular level. OPLS-AA force-field parameters used in the simulations were reported previously for $[EMIM]^+$,[12b] whereas those for LAC^- are shown in Table S4 (Supporting Information). To validate the reported force-field parametrization, and thus to ensure the reliability of structural features inferred from the simulations, calculated properties were compared with experimental ones. In Figure 7, density and isobaric thermal expansivity comparisons are reported as a function of temperature. Simulated densities are always lower than experimental ones with deviations of roughly 2.0% (Figure 7a). This level of agreement is in the same range as literature studies on different ionic liquids[75] or recent parametrizations on lactate-containing ionic liquids.[76] Predictions of the isobaric thermal expansivity, α_P, allow inferring if the simulations are able to capture the changes in density with temperature at constant pressure. α_P was predicted from the simulations using the well-known fluctuation equations in the NPT ensemble.[75a] Predictions of α_P show deviations of roughly 14% (Figure 7b); although these deviations may seem too large, they are in the range of literature predictions,[75a,b] considering the difficulty in predicting accurately derived thermodynamic properties such as α_P. Nevertheless, the trend of the property is captured well by the simulation, and thus, the degree of agreement of the studied properties over the considered temperature range is reasonable and should allow inferring reliable insights into the liquid properties and structural features for [EMIM]LAC.

Lactate anion has two main molecular sites through which it may interact: the hydroxyl group and the carbonyl site. A relevant aspect is if hydroxyl and carbonyl groups are in plane (and thus intramolecular hydrogen bonding may be developed) or out of plane (and intramolecular hydrogen bonding is hindered). Previous results for the related molecular solvent ethyl lactate[14] have showed that the hydroxyl group is clearly out of plane, and thus relevant dihedral angles for LAC^- anion are studied in this work to support this behavior in [EMIM]LAC. Results reported in Figure 8 show that hydroxyl and carbonyl groups are not in plane.

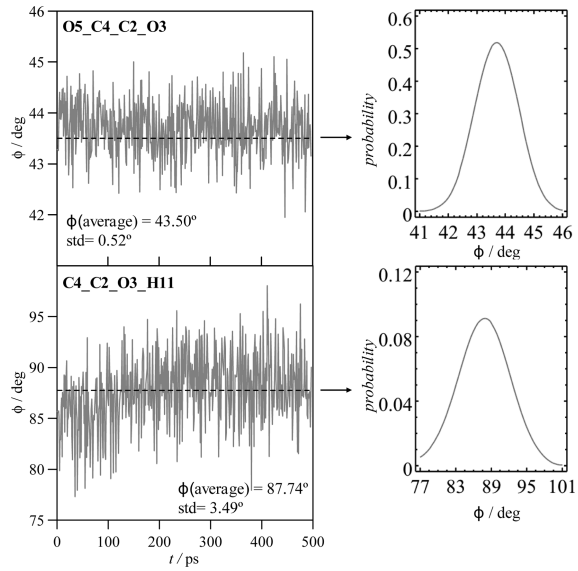

Figure 8. Time evolution of the selected dihedral angles, in LAC^- anion for the last 500 ps of the molecular dynamics simulations of [EMIM]LAC at 298 K and 0.1 MPa. Atom numbering as in Table S4 (Supporting Information). Probability plots are also reported for each dihedral and average and standard deviation, std, values. Dashed lines show average values.

Structural features are analyzed using radial distribution functions, RDFs; plots for selected pairs are reported in Figure 9. Anion/anion interactions are analyzed using the H11_O3 (hydroxyl/hydroxyl interaction) and H11_O5 (hydroxyl/carbonyl interaction). Although a certain degree of structuring may be inferred from the two wide peaks reported in Figure 9a, the maxima for these peaks appear at long distances (~7 and 14 Å), and thus the LAC^-/LAC^- interaction should not be very remarkable. Cation/cation interactions are analyzed in Figure 9b; the structuring is almost absent and the RDF values lower than 1 for $r < 6$ Å show that $[EMIM]^+$ cations are absent from the first solvation spheres of cations. The most remarkable results for cation/anion interaction are shown in Figure 9c. $[EMIM]^+$ has two main positions through which it may interact with LAC^- anion: (i) the acidic hydrogen between both nitrogens, H19, and (ii) the hydrogens in the opposite position in the $[EMIM]^+$ cation, H17 and H18. Results show that interaction with both positions is almost equivalent; moreover, the larger peaks for interactions through the carbonyl oxygen show that anion interaction with the cation may be developed both through H19 and H17/H18 sites but preferentially through the carbonyl group. Another question arises from the presence of alkylic groups in the studied ions, and thus the possibility of developing apolar domains within the ionic liquids;[77] results in Figure 9d show a certain degree of apolar arrangement with successive solvation spheres separated ~4 Å, and with a first narrow peak, more intense for the interaction between alkyl chains of anion/cation, C1_C20 and C1_C27, than for cation/cation, C27_C27. This apolar arrangement may arise from the interaction of anions surrounding cations that leads to proximity of alkylic chains of both ions. Another remarkable feature to characterize anion/cation interaction is the way in which LAC^- anions are placed around the $[EMIM]^+$: the representative snapshot reported in Figure 10 shows that four LAC^- anions surround a single $[EMIM]^+$ cation, two of them through the H17/H18 position (one for each hydrogen) and the remaining two ones simultaneously through the H19 position. Moreover, this molecular graph shows that LAC^- anion and $[EMIM]^+$ are almost in plane.

The temperature effect on the [EMIM]LAC structure is analyzed through the evolution of RDFs for the O5_H19 and O5_17 pairs with variable temperature [Figure S4 (Supporting Information)]. The reported results show a certain weakening of anion/cation interaction with increasing temperature, as may be expected; nevertheless, this effect is not very important for the studied temperature range.

The vaporization enthalpy, ΔH_{vap}, is a very important property because of its relationship with intermolecular forces; it is calculated from molecular dynamics simulations according to eq 4:[78]

$$\Delta H_{vap} = \Delta U_{L,G} + RT = (U_{G,inter} - U_{L,inter}) + (U_{G,intra} - U_{L,intra}) + RT \quad (4)$$

where U stands for the molar internal energy of the liquid, L, and gas, G, phases. The subscripts "intra" and "inter" refer to intramolecular (bond, angle, and dihedral contributions together with nonbonded intramolecular interactions) and intermolecular (Coulombic and van der Waals interactions) contributions to the internal energy. To calculate properties for the gas phase, a single ionic pair was simulated.[78,79] The analysis of molecular simulations results allows splitting the different contributions to the vaporization enthalpy (Table 1). The absence of experimental ΔH_{vap} data for [EMIM]LAC does not allow any comparison with predicted values. The results show that intramolecular and kinetic contributions to the vaporization enthalpy are almost negligible, and thus, the two main contributions to this property are Coulombic and van der Waals forces, with contributions of ~75 and 25% for [EMIM]LAC, respectively. These results are in agreement with previous calculations for imidazolium-containing liquids.[78]

Finally, to analyze the temperature effect on the intermolecular forces present in liquid [EMIM]LAC, the intermolecular (interionic) interaction energy, E_{inter}, is calculated as a function of temperature (Figure 11). Calculated E_{inter} values are remarkably large, which is in agreement with the viscosity values reported in the previous section. The temperature effect on this energy is not very remarkable for the studied range, decreasing in an almost linear fashion ~7%, in absolute value, on going from 283 to 343 K.

3.2. [EMIM]LAC + Water Mixtures. The analysis of the molecular level effects upon mixing of the studied ionic liquid with water is of remarkable importance because of the complexity arising from the simultaneous presence of hydrogen bonding and Coulombic and van der Waals forces in the mixture, together with the changing degrees of aggregation of the ions with dilution in the cosolvent.[80,81]

3.2.1. Spectroscopic Measurements. DRS results for water + [EMIM]LAC mixed fluids were analyzed as a function of composition, at 298.15 K, using two Debye processes as previously done for pure [EMIM]LAC (Table S5 in the Supporting Information). A bimodal relaxation time distribution using two Debye processes was used in the whole composition range. For pure water, two relaxation times at 8.38 and 1.1 ps were considered according to Buchner et al.;[82] the faster relaxation process lies well above the higher frequency limit of this work (8.8 ps at 18.09 GHz and 1.1 ps at 144.69 GHz), so only the slower relaxation time is considered in this work. This relaxation process appearing at 8.8 ps reflects the cooperative dynamics of the hydrogen bonding network in liquid water.[82] Results for water + [EMIM]LAC mixed fluids are reported in Figure S5 (Supporting Information) as a function of [EMIM]-

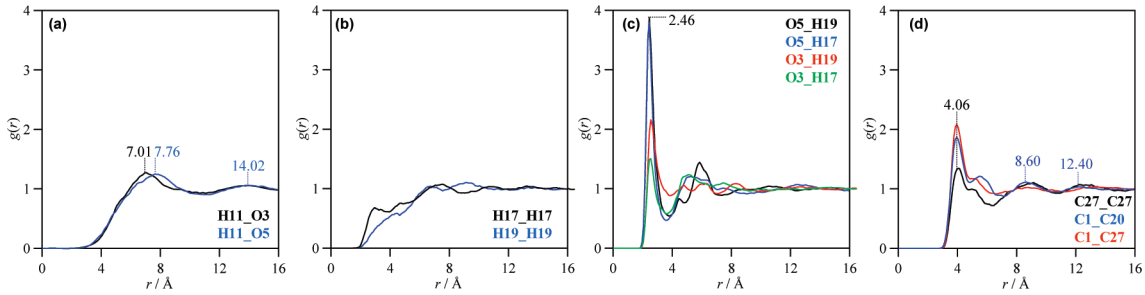

Figure 9. Site−site radial distribution functions, $g(r)$, for [EMIM]LAC calculated from molecular dynamics simulations at 298 K and 0.1 MPa. Atom numbering as in Table S4 (Supporting Information). Numerical values within each panel show intersite distances for selected maxima.

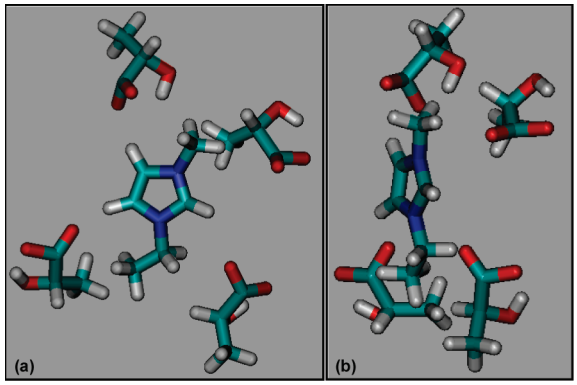

Figure 10. Snapshot obtained from molecular dynamics simulations for [EMIM]LAC at 298.15 K and 0.1 MPa. The figure shows the LAC^- anions surrounding a selected $[EMIM]^+$ cation within the first solvation shell ($r = 3.6$ Å obtained from the first minima in Figure 9c for O5_H17 and O5_H19 pairs). Color code: red, oxygen; blue, nitrogen; dark gray, carbon; light gray, hydrogen.

TABLE 1: Molecular Dynamics Simulated Enthalpies of Vaporization, ΔH_{vap}, and Differences between Liquid and Gas Phase Values for the Coulomb, Lennard-Jones (van der Waals), Intramolecular, and Kinetic Energies of [EMIM]LAC at 298.15 K and 0.1 MPa[a]

ΔH_{vap}	Coulomb	van der Waals	intramolecular	kinetic	RT
134.40	96.26	32.14	2.78	0.74	2.48

[a] All values in kJ mol^{-1}.

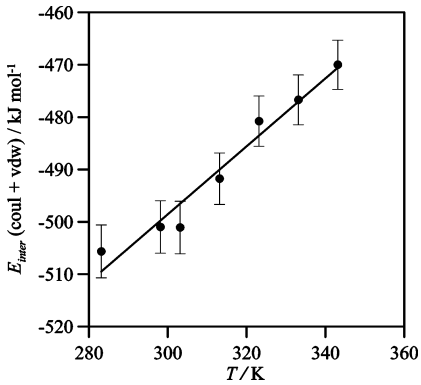

Figure 11. Intermolecular interaction energy, E_{inter} (Coulombic + van der Waals), from molecular dynamics simulations for liquid [EMIM]-LAC at 0.1 MPa as a function of temperature.

LAC mole fraction. The composition evolution of the fitting parameters is reported in Figure 12, and it may be inferred a physically reasonable behavior. The behavior of the static dielectric constant, ε_s, together with the derived mixing property, $\Delta\varepsilon_s$, obtained according to a method previously reported,[29] is reported in Figure 12a. A strongly nonlinear trend for ε_s is obtained leading to large negative values of $\Delta\varepsilon_s$, with a minimum at ∼0.3 [EMIM]LAC mole fraction. This behavior points to an effective interaction between water and [EMIM]-LAC ions leading to a reduction of the effective dipole moments because of this interaction. The behavior of dc conductivity obtained both from experimental measurements and from DRS data analysis shows interesting features (Figure 12b): a maximum in this function for $x\sim 0.05$ is obtained, which may be explained considering the increase of mobile ion density upon addition of [EMIM]LAC to pure water, and the further decrease of conductivity with larger [EMIM]LAC concentration is because of the association of ion pairs. Nevertheless, if conductivity data are compared with those for $[EMIM]BF_4$,[83] a different behavior is obtained because of the presence of the LAC^- anion; whereas for $[EMIM]BF_4$ the maximum of dc conductivity function appears for ∼0.1 ionic liquid mole fraction and the value of the maximum is ∼90 mS cm^{-1}, the values for [EMIM]LAC are less than half of these and the further decrease with increasing ionic liquid mole fraction is more steep. Thus the trend to form ion pairs in LAC^- containing ionic liquids is more remarkable. The behavior of the relaxation amplitudes and times for the two Debye processes considered in the 200 MHz−20 GHz frequency range is reported in Figure 12c,d. The slower relaxation process remains in the 130−190 ps range for all studied compositions, with a not well-defined maximum for the 0.2−0.6 [EMIM]LAC mole fraction range. The relaxation amplitude of this process evolves through a maximum for $x \sim 0.1$. The second and slower process shows a maximum in its relaxation time at $x \sim 0.12$ and its amplitude shows two clearly defined linear regions separated by $x \sim 0.12$; for lower mole fractions the amplitude decreases in a steep way and for larger mole fractions it is almost constant. The slower process may be assigned to reorientation of cations and also to anions present in the mixture, for water-rich mixtures ($x < 0.1$) free ions prevailing in the solution, and thus the amplitude of this process increases with increasing ionic liquid concentration up to a value of x for which formation of ionic pairs leads to a decrease in the amplitude. The formation of these pairs should lead to slower relaxations which would justify the broad maximum for this process reported in Figure 12d. The second process should reflect the properties of ionic liquid interacting with water molecules. The relaxation process for pure water appears at 8.8 ps and for pure [EMIM]LAC at 13.86 ps, and thus an overlapping in this region is inferred. For water-rich regions, this second process should reflect the effect of ions on water cooperative dynamics for the hydrogen bonding network. The shifting of relaxation time toward slower values, with a maximum at $x \sim 0.12$ of ∼21 ps (2.4 times the value for pure water) shows a remarkable interaction between water and ionic liquid; as this process is mainly related to the anion rotation, the interaction between water and the ionic liquid should be

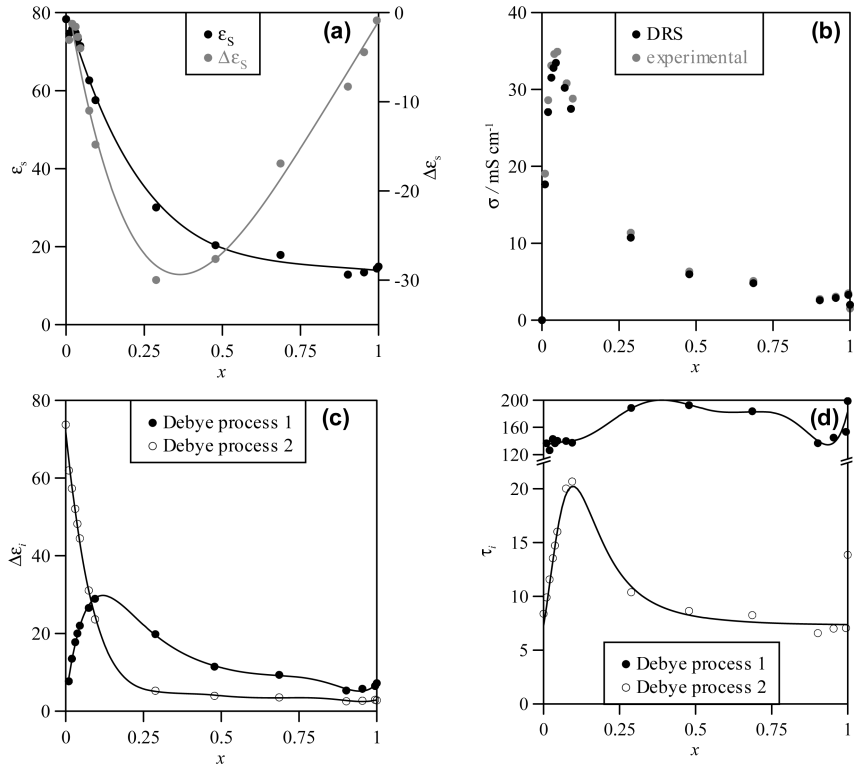

Figure 12. (a) Static dielectric constant, ε_s, and mixing static dielectric constant, $\Delta\varepsilon_s$, (b) conductivity, σ, experimental values compared with those calculated from DRS measurements, (c) relaxation amplitudes, $\Delta\varepsilon_i$, and (d) relaxation times, τ_i, obtained from the fit of experimental dielectric spectra according to two Debye processes, for x[EMIM]LAC + (1 − x)water binary mixtures at 298.15 K and 0.1 MPa. (—) Polynomial fittings for guiding purposes.

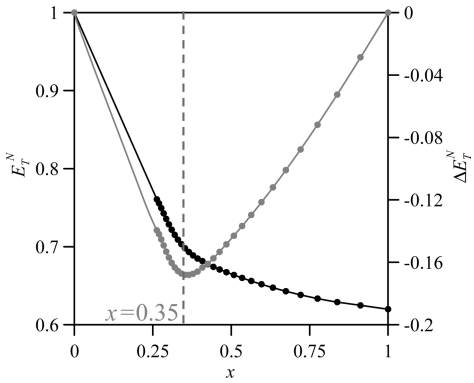

Figure 13. Normalized Reichardt's parameter, E_T^N, and mixing normalized Reichardt's parameter, ΔE_T^N, in [EMIM]LAC + (1 − x)-water mixed fluids at 298.15 K and 0.1 MPa. Points show experimental data and continuous lines for guiding purposes. Dashed line shows the separation between the two zones (see text for explanation). Experimental data are reported only for x > 0.25 because of indicator insolubility in water-rich mixtures.

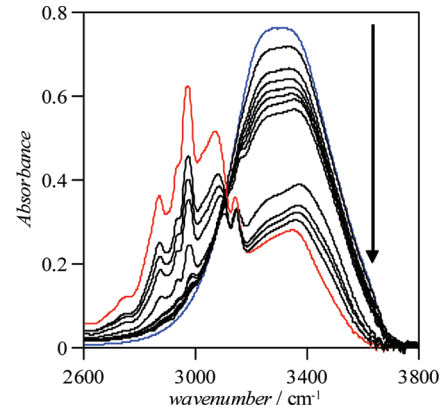

Figure 14. ATR-FTIR spectra for x[EMIM]LAC + (1 − x)water mixed fluids at 298.15 K and 0.1 MPa. Blue line shows results for pure water and red line shows results for pure [EMIM]LAC. Arrow shows increasing [EMIM]LAC mole fraction, from top to bottom: 0, 0.0097, 0.0197, 0.0304, 0.0374, 0.0453, 0.0739, 0.0940, 0.2881, 0.4781, 0.6868, 0.8968, and 1.

carried out through LAC^- anions. The sudden change in the properties of the slow relaxation process, in both its amplitude and time, for x > 0.12, shows that once ionic pairs begin to form with increasing ionic liquid mole fraction, the interaction with water is clearly hindered because it may be developed mainly through anions which are occupied in the pairs. This behavior is in agreement with the scheme proposed by Dupont[80] for the structural changes rising from the dilution of an ionic liquid in a cosolvent such as water.

Solvatochromic results using Reichardt's dye are reported in Figure 13 and Table S6 (Supporting Information). Although, as it has been reported in previous sections, solvatochromic parameters are not an accurate indicator of solvent polarity for ionic liquid containing fluids, results reported in Figure 13 show clearly two regions for [EMIM]LAC + water mixtures, whereas for x > 0.35 the mixed fluid polarity remains almost constant and close to the value of pure [EMIM]LAC for values x < 0.35 the fluid polarity increases remarkably. These results show that [EMIM]LAC maintains its structure up to highly diluted regions, and for water rich regions ions are mainly nonassociated and interacting with water molecules, disrupting the water hydrogen bonding network and decreasing medium polarity. These results are very close to those previously reported for the related ethyl lactate + water mixed fluid,[53] and thus, it shows that the interaction between the ionic liquid and water molecules is developed through the LAC^- anion. These results are also in

TABLE 2: Gaussian−Lorentzian Parameters for ATR-FTIR Spectral Fit for x[EMIM]LAC + (1 − x)Water Mixtures at 298.15 K and 0.1 MPa[a]

		I				II				III				IV				
x	M	ν/cm^{-1}	amplitude	fwhm	area	ν/cm^{-1}	amplitude	fwhm	area	ν/cm^{-1}	amplitude	fwhm	area	ν/cm^{-1}	amplitude	fwhm	area	A_I/A_{II}
0.0000	63.0	3218.3	0.6060	263.6	190.5	3398.5	0.5041	237.6	127.5	3550.6	0.1013	122.4	13.2	3625.3	0.0516	75.2	4.1	1.49
0.0097	50.7	3239.0	0.4899	180.0	99.2	3373.0	0.5126	174.9	99.3	3500.7	0.2832	173.1	54.2	3611.0	0.0637	105.2	7.1	1.00
0.0197	46.7	3249.2	0.4033	157.7	74.2	3372.1	0.4840	164.7	85.5	3499.0	0.2740	161.9	47.2	3610.7	0.0673	104.8	7.5	0.87
0.0304	42.9	3248.0	0.4098	157.0	72.9	3373.4	0.4775	164.7	83.7	3501.2	0.2677	162.4	46.3	3613.0	0.0617	106.1	7.0	0.87
0.0374	40.8	3246.9	0.4018	157.4	71.7	3373.6	0.4631	165.1	81.6	3501.4	0.2614	164.2	45.7	3613.6	0.0557	105.3	6.2	0.88
0.0453	38.5	3250.4	0.4140	151.0	67.8	3373.6	0.4613	155.5	76.4	3493.9	0.2745	154.8	45.2	3604.8	0.0731	115.6	9.0	0.89
0.0739	31.9	3248.4	0.4085	150.8	67.4	3374.4	0.4574	156.1	76.0	3495.1	0.2704	153.8	44.3	3604.4	0.0639	113.2	7.7	0.89
0.0940	28.2	3245.2	0.4081	149.7	66.4	3371.1	0.4469	155.9	75.9	3491.6	0.2601	152.7	43.2	3600.8	0.0608	111.1	6.3	0.88
0.2881	11.5	3247.1	0.2742	141.3	41.2	3370.8	0.3090	145.0	47.7	3479.8	0.2057	141.5	31.0	3577.3	0.0485	123.7	2.9	0.86
0.4781	5.7	3236.8	0.2413	148.9	38.2	3367.0	0.2759	148.4	43.6	3476.5	0.1630	139.8	24.3	3564.1	0.0389	132.1	5.5	0.88
0.6862	2.5	3238.2	0.2178	146.9	34.1	3367.2	0.2540	149.8	41.3	3475.0	0.1388	145.3	23.7	3545.4	0.0338	137.5	5.8	0.82
0.8968	0.6	3246.2	0.2091	135.4	30.1	3366.8	0.2525	137.5	37.0	3476.3	0.1384	131.0	19.3	3567.6	0.0243	104.6	2.7	0.81
1.0000	0.0	3223.0	0.2197	158.5	31.0	3354.8	0.2198	152.3	35.6									

[a] M stands for water molarity (mol dm^{-3}).

agreement with literature values for imidazolium containing ionic liquids.[84]

ATR-FTIR results are reported in Figure 14. The spectral region over 2600−3800 cm^{-1} is the most useful one because of the presence of OH-stretching bands in water and LAC$^-$ anion. The proximity between water and LAC$^-$ OH bands makes difficult the deconvolution process; moreover, the assignment of pure water bands in the OH-stretching region is controversial in the literature.[85] This deconvolution is commonly carried out using four bands, named I to IV in increasing wavenumber. The first one, I, is assigned to fully hydrogen bonded molecules for tetrahedrally coordinated water; the second one, II, is assigned to fully hydrogen bonded molecules but not fully coordinated. Bands III and IV correspond to molecules not fully hydrogen bonded, III for OH oscillator hydrogen bonded and IV for not hydrogen bonded.[85] Band I is frequently called the *icelike* peak,[86] because it shows a well-ordered structure, whereas band II is called *liquidlike*[86] and represents a more disordered structure; thus the relationship between the areas of both bands, A_I/A_{II}, is important for analyzing the structure in liquid water hydrogen bonding networks and the effect of the addition of other species, such as [EMIM]LAC in this work. Some authors have reported A_I/A_{II} values of around 4,[86] and thus peak I clearly prevails over II, whereas other authors show values in the 1.10−1.20 range,[85,87] and thus although I prevails, peak II is also very remarkable. Deconvolution results obtained in this work are reported in Table 2; values for pure water show peaks maxima in agreement with literature values.[85−87] The A_I/A_{II} ratio is 1.5 in agreement with some literature[85,87] and clearly lower than the values reported by Jeon et al.[86] The results show how upon addition of small quantities of [EMIM]LAC the water hydrogen bonding network is disrupted and A_I/A_{II} decreases abruptly below 1, thus leading to a more disordered structure because of the prevailing liquidlike peak. Nevertheless, when the [EMIM]LAC concentration increases, the ratio A_I/A_{II} remains almost constant (∼0.9), and thus [EMIM]LAC does not remarkably disrupt the water network because of the presence of the OH group in the LAC$^-$ anion that allows development of hydrogen bonds with water molecules. LAC$^-$ OH groups lead to peaks that overlap with those from water molecules; the low-frequency peak could be assigned to hydrogen bonded OHs, whereas the high-frequency one could be assigned to free OH groups. For [EMIM]LAC-rich mixtures the addition of water does not change remarkably the spectral features of the ionic liquid; thus [EMIM]LAC preserves its structure up to high dilution.

3.2.2. Thermophysical Properties. These properties are reported in Table S7 (Supporting Information) and Figure 15. The results for density, refractive index, and isentropic compressibility show two clearly defined regions with increasing [EMIM]LAC mole fraction: (i) a steep variation of the properties from the values of pure water up to $x \sim 0.1-0.25$ and (ii) a region from $x \sim 0.25$ up to pure [EMIM]LAC for which properties are almost constant.

The increase of density with the addition of [EMIM]LAC to pure water on going from $x = 0$ to ∼0.25 shows that, although the ionic liquid disrupts the liquid water structure, through the interaction with water molecules it leads to an efficient packing. Moreover, the negative excess volume in the whole composition range, with a minimum at $x \sim 0.25$, shows this efficient packing. Therefore, these density-derived results show that, for low [EMIM]LAC mole fractions, isolated ions interact with water molecules, probably though hydrogen bonding, leading to very effective solvations, whereas once the [EMIM]LAC concentration is large enough ion pairing dominates the fluid structuring. This is in agreement with the refractive index and isentropic compressibility behavior reported in Figure 15c,d, and this last property shows even more pronounced changes with [EMIM]-LAC mole fraction. Excess isentropic compressibility (Figure 15c) shows a sharp minimum for $x = 0.1$, thus showing that for this concentration the less compressible mixed fluid is obtained; probably from $x = 0$ to ∼0.1 free ions will dominate in the fluids and from $x = 0.1$ to ∼0.25 ionic pairs will begin to be more abundant leading to void spaces within the fluid which would make it more compressible. It should be noted that the values of excess and mixing properties reported in Figure 15 are remarkably large in comparison with other ionic liquid/water mixtures,[88] and thus, a stronger interaction of LAC$^-$ anions with water molecules may be inferred.

As previously reported in the literature for several ionic liquids,[61,89] water has a strong effect on [EMIM]LAC viscosity, decreasing with increasing water mole fraction. This could be considered a technological advantage: if [EMIM]LAC ionic liquid maintains most of its structure upon water dilution but at the same time viscosity decreases remarkably with increasing water concentration, [EMIM]LAC + water mixtures could be used for industrial applications preserving the properties of pure ionic liquid and at the same time having viscosities close to those of common organic solvents. Mixing viscosity is negative in the whole composition range, with a minimum for ∼0.70 [EMIM]LAC, and thus mixing always leads to a less viscous system than the linear combination of the values of both pure fluids, which is more remarkable for [EMIM]LAC-rich mixtures. The large effect of water on ionic liquid viscosity is still not fully understood.[61,89] Water has two main properties: (i) large dielectric constant and (ii) ability to develop hydrogen bonding.

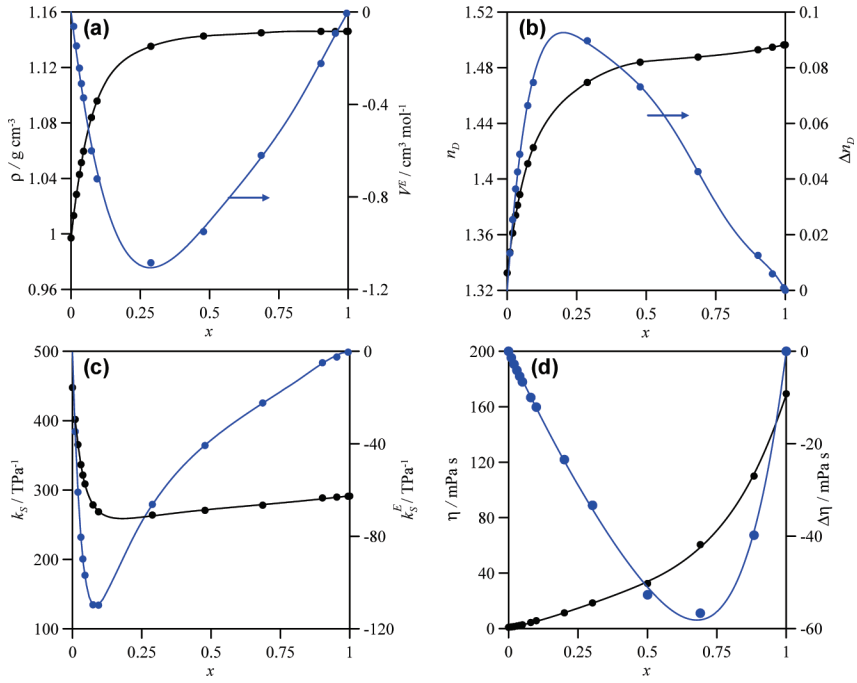

Figure 15. Thermophysical properties for x[EMIM]LAC + (1 − x)water mixed fluids at 298.15 K and 0.1 MPa. x stands for mole fraction, ρ stands for mass density, V^E stands for excess molar volume, n_D stands for refractive index for the sodium D line, Δn_D stands for the mixing refractive index, k_S stands for isentropic compressibility, and k_S^E stands for excess isentropic compressibility. Solid circles show experimental data, continuous lines are for guiding purposes, and dashed lines show the two regions in the fluids' behavior.

The large dielectric constant of water should weaken the electrostatic interactions between the ions when water is added to pure [EMIM]LAC; this should be an expansive effect on mixture volume and lead to a decrease in viscosity. The ability of water to develop hydrogen bonding together with the presence of hydroxyl and COO^- groups in LAC^- cation should lead to very effective interactions between the anion and water molecules; this should be a contractive effect on volume and lead also to a decrease in viscosity because hydrogen bonds should be weaker than ion/ion electrostatic interactions. Hence, both effects could explain the decrease in viscosity upon water addition to pure [EMIM]LAC, but the negative excess molar volume reported in Figure 15a shows that the formation of hydrogen bonding between water and [EMIM]LAC, mainly through the anion, are more important than the disruptive effect of water molecules rising from its large polar character.

3.2.3. Molecular Dynamics Simulations. The force-field parametrization used for [EMIM]LAC + water mixtures [the OPLS-AA parameters reported in Table S4 (Supporting Information) for the ionic liquid and SPC-E for water] is analyzed by comparison of experimental density values with those predicted from the simulations; see Figure 16. The molecular dynamics predictions accurately capture the complex behavior of this complex mixture, with better accuracy for water-rich mixtures.

Structural features in the mixed fluids are analyzed using radial distribution functions, RDFs, which are reported for selected pairs in Figure 17 as a function of mixture composition for isobaric/isothermal conditions. Association between anion and cation in a mixture is analyzed through the O5_H19 pair (carbonyl oxygen in the LAC^- anion−hydrogen in the imidazolium ring of the cation placed between nitrogens), water−water homoassociation through the OW_HW pair, and heteroassociation between water and anions through the O5_HW pair. RDFs for the O5_H19 pair show a first remarkable peak at 2.46 Å (Figure 17a); this position remains constant with increasing

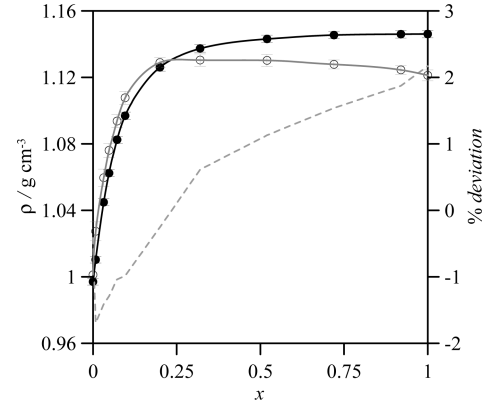

Figure 16. Experimental and calculated (molecular dynamics simulations with parameters reported in Table S4, Supporting Information, for [EMIM]LAC and SPC-E for water) density, ρ, for x[EMIM]LAC + (1 − x)water mixed fluids at 298.15 K and 0.1 MPa. Filled circles, experimental values; empty circles, molecular dynamics values; continuous lines, guiding lines; gray dashed line, percentage deviations.

water mole fraction. The intensity of this peak decreases with increasing water mole fraction, as may be expected because of the dilution of anions in the surrounding water medium, but it shows remarkably large values up to very high dilution levels. The intensity of the first peak for O5_H19 RDF for $x = 0.20$ is 58% of the value for pure [EMIM]LAC, and thus, it confirms that the studied ionic liquid maintains a high degree of structuring, through the cation/anion interaction, up to very high dilution levels. The second broad and weak band at ∼5.8 Å vanishes with increasing water mole fraction, thus pointing to the development of isolated cation/anion pairs embedded in a water medium.

The interaction between water molecules from the OW−HW RDFs shows the two characteristic peaks at 1.80 and 3.25 Å (Figure 17b). The positions of the maxima for these peaks do not change with increasing [EMIM]LAC mole fraction, but their

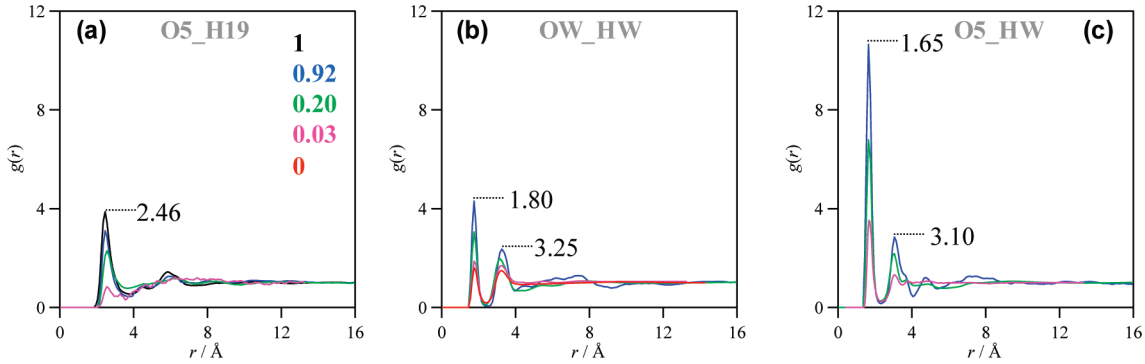

Figure 17. Site−site radial distribution functions, $g(r)$, for x[EMIM]LAC + (1 − x)water mixed fluids, calculated from molecular dynamics simulations at different concentrations at 298 K and 0.1 MPa. x = [EMIM]LAC mole fraction. Values within panel a show the color code for different values of x. Atom numbering as in Table S4 (Supporting Information). OW and HW stand for water oxygen and hydrogen, respectively.

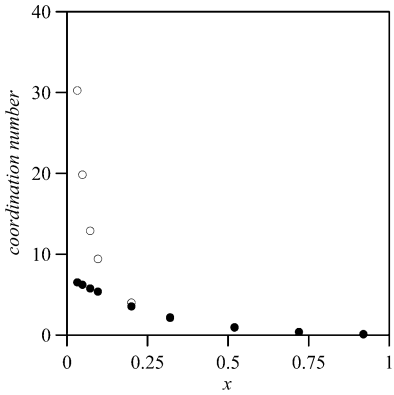

Figure 18. Simulated, molecular dynamics at 298 K and 0.1 MPa, coordination number of water around LAC^- anions, solid circles, in comparison with molar ratio of water molecules to [EMIM]LAC, empty circles. Simulated values obtained from RDFs are reported according to a previously reported procedure,[90] integrating functions up to 4.00 Å.

amplitudes are larger, which points to an enhancing effect of the ionic liquid on water structuring. Therefore, it may be concluded that [EMIM]LAC interactions do not change remarkably with water dilution, up to very high dilution levels, and W structure is clearly reinforced by the presence of ions.

Results reported in Figure 17c for the O5_HW pair show remarkable hydrogen bonding between the ionic liquid and water molecules, because of the sharp first two peaks, whose maxima at 1.65 and 3.10 Å point to at least two well-defined solvation spheres. Coordination numbers of water around the anion, obtained from RDFs for the O5_HW pair,[90] are reported in Figure 18 in comparison with the molar ratio of water to anions. Values of the coordination number increase with increasing mole fraction and resemble those values of the water/anion mole ratio up to water mole fraction ∼ 0.80; from that mole fraction the calculated coordination number is remarkably lower than the mole ratio, thus pointing to a prevailing role of water−water interactions from that concentration, whereas for larger ionic liquid concentrations water−anion interactions are more important. This behavior of the coordination number is in agreement with those reported in the literature for other aqueous solutions of ionic liquids.[91]

4. Concluding Remarks

The combined experimental/computational study reported in this work on [EMIM]LAC, pure and water mixed, allows extraction of several relevant conclusions:

(i) [EMIM]LAC is a moderately polar fluid with a strong affinity for water.

(ii) DRS allows a good characterization of ionic liquid polarities, which leads to reliable results in contrast to other techniques based in the behavior of dyes of ATR spectra of certain solutes such as water.

(iii) The presence of the hydroxyl and carbonyl groups in the LAC^- anion allows a strong interaction with the $[EMIM]^+$ cation.

(iv) The analysis of thermophysical properties allows characterization of [EMIM]LAC as a moderately viscous fluid, with high ionicity.

(v) The van der Waals forces develop an important role in the structure of this fluid.

(vi) [EMIM]LAC is able to maintain a high degree of structuring upon water dilution up to very high dilution levels.

(vii) The ionic liquid has a strong effect on water structuring, and it seems to interact very effectively with water molecules through hydrogen bonding, thus reinforcing the hydrogen bonding network.

(viii) The effect of water on [EMIM]LAC structuring is not very remarkable: the ionic liquid maintains its structure and the fluid viscosity decreases. Thus, water could be used to tune the mixed fluid physical properties while maintaining the main structural features of the pure ionic liquid.

Supporting Information Available: Table S1 (parametrization of DRS spectra for pure [EMIM]LAC), Figure S1 (molecular structures of $[EMIM]^+$ and LAC^- ions), Table S2 (results for Reichardt's dye in [EMIM]LAC), Figure S2 (ATR-FTIR spectrum in the OH-stretching region of 1 wt % water solution in [EMIM]LAC), Figure S3 (increase of mass as a function of time for dried [EMIM]LAC exposed to atmosphere), Table S3 (thermophysical properties of [EMIM]LAC), Table S4 (OPLS-AA force field parameters for LAC^- ion), Figure S4 (effect of temperature on selected RDFs for [EMIM]LAC), Figure S5 (DRS spectra for x[EMIM]LAC + (1 − x)water mixed fluids), Table S5 (parametrization of experimental dielectric spectra for x[EMIM]LAC + (1 − x)water mixed fluids), Table S6 (Reichardt's dye in x[EMIM]LAC + (1 − x)water mixed fluids) and Table S7 (thermophysical properties of x[EMIM]LAC + (1 − x)water mixed fluids). This material is available free of charge via the Internet at http://pubs.acs.org.

References and Notes

(1) (a) *Ionic Liquids as Green Solvents. Progress and Prospects*; Rogers, R. D., Seddon, K. R., Eds.; ACS Symposium Series 856; American

Chemical Society: Washington, DC, 2003. (b) *Electrochemical Aspects of Ionic Liquids*; Ohno, H., Ed.; Wiley: Hoboken, NJ, 2005. (c) *Ionic Liquids in Polymer Systems: Solvents, Additives, and Novel Applications*; Brazel, C. S., Rogers, R. D., Eds.; ACS Symposium Series 913; American Chemical Society: Washington, DC, 2003. (d) *Ionic Liquids in Synthesis*; Wasserscheid, P., Welton, P., Eds.; Wiley-VCH: Weinheim, 2007. (e) *Ionic Liquids IV: Not Just Solvents Anymore*; Brennecke, J. F., Rogers, R. D., Seddon, K. R., Eds.; ACS Symposium Series 975; American Chemical Society: Washington, DC, 2007. (f) Koel, M. *Ionic Liquids in Chemical Analysis*; CRC Press: Boca Raton, 2008. (g) Kirchner, B. *Ionic Liquids*; Topics in Current Chemistry; Springer: Berlin, 2009. (h) Zhang, S.; Lu, X.; Zhou, Q.; Li, X.; Zhang, X. *Ionic Liquids: Physicochemical Properties*; Elsevier: New York, 2009.

(2) (a) Davis, J. H.; Fox, P. A. *Chem. Commun.* **2003**, 1209. (b) Plechkova, N.; Seddon, K. R. Ionic Liquids: "Designer" Solvents for Green Chemistry. In *Methods and Reagents for Green Chemistry*; Tundo, P., Perosa, A., Zecchini, F., Eds.; Wiley: Hoboken, NJ, 2007. (c) Rogers, R. D. *Nature* **2007**, *447*, 917.

(3) (a) Gathergood, N.; García, M. T.; Scammells, P. J. *Green Chem.* **2004**, *6*, 166. (b) Bernot, R. J.; Buesecke, M.; Evans-White, M. A.; Lamberti, G. A. *Environ. Toxicol. Chem.* **2005**, *24*, 87. (c) Pretti, C.; Chiappe, C.; Pieraccini, D.; Gregori, M.; Abramo, F.; Monni, G.; Intorre, L. *Green Chem.* **2006**, *8*, 238. (d) Zhao, D.; Liao, Y.; Xhang, Z. *Clean* **2007**, *35*, 42. (e) Stolte, S.; Abdulkarim, S.; Arning, J.; Blomeyer, A.; Bottin, U.; Matzke, M.; Ranke, J.; Jarstoff, B.; Thöming, J. *Green Chem.* **2008**, *10*, 214.

(4) (a) Davis, J. H. *Chem. Lett.* **2004**, *33*, 1072. (b) Lee, S. *Chem. Commun.* **2006**, 1049. (c) Fei, Z.; Geldach, T. J.; Zhao, D.; Dyson, P. J. *Chem.—Eur. J.* **2006**, *12*, 2122. (d) Hnioka, S.; Maruyama, T.; Sotani, T.; Teramoto, M.; Matsuyama, H.; Nakashima, K.; Hanaki, M.; Kubota, F.; Goto, M. *J. Membr. Sci.* **2008**, *314*, 1. (e) Huang, J.; Riisager, A.; Berg, R. W.; Fehrmann, R. *J. Mol. Catal. A: Chem.* **2008**, *279*, 170.

(5) Holbrey, J. D.; Seddon, K. R. *Clean Prod. Process.* **1999**, *1*, 223.

(6) (a) de Andrade, J.; Boes, E. S.; Stassen, H. In *Ionic Liquids IIIA: Fundamentals, Progress, Challenges, and Opportunities, Properties and Structure*; Rogers, R. D.; Seddon, K. R., Eds.; ACS Symposium Series 901; American Chemical Society: Washington, DC, 2005; p 118. (b) Lopes, J. N. C.; Deschamps, J.; Padua, A. A. H. In *Ionic Liquids IIIA: Fundamentals, Progress, Challenges, and Opportunities, Properties and Structure*; Rogers, R. D., Seddon, K. R., Eds.; ACS Symposium Series 901; American Chemical Society: Washington, DC, 2005; p 134. (c) Rey, C.; Tormo, A. L.; Vega, L. F. *Fluid Phase Equilib.* **2006**, *256*, 62. (d) Hardacrem, C.; Holbrey, J. D.; Nieuwenhuyzen, M.; Youngs, T. G. A. *Acc. Chem. Res.* **2007**, *40*, 1146.

(7) Marsh, K. N.; Deev, A.; Wu, A. C. T.; Tran, E.; Klamt, A. *Korean J. Chem. Eng.* **2002**, *19*, 357.

(8) Swatloski, R. P.; Holbrey, J. D.; Rogers, R. D. *Green Chem.* **2003**, *5*, 361.

(9) (a) *Handbook of Pharmaceutical Salts. Properties, Selection and Use*; Stahl, P. H., Wermuth, C. G., Eds.; Wiley-VCH: Weinheim, 2002. (b) Office of the Federal Register. *Code of Federal Regulations. Food and Drugs, Chapter 21, part 184. Direct Food Substances Affirmed As Generally Recognized As Safe*; U.S. Government Printing Office: Washington, DC. Available: http://ecfr.gpoaccess.gov/cgi/t/text/text-idx?c=ecfr&sid=786bafc6f6343634fbf79fcdca7061e1&rgn=div5&view=text&node=21:3.0.1.1.14&idno=21 (accessed June 27, 2009).

(10) (a) Renner, R. *Environ. Sci. Technol.* **2001**, *35*, 410. (b) Wagner, M.; Uerdingen, M. In *Multiphase Homogeneous Catalysis*; Cornils, B., Herrmann, W. A., Horvath, I. T., Leitner, W., Mecking, S., Olivier-Bourbigou, H., Vogt, D., Eds.; Wiley-VCH: Weinheim, 2005. (c) Wassersheid, P.; Haumann, M. In *Catalyst Separation, Recovery and Recycling: Chemistry and Process Design*; Cole-Hamilton, D. J., Tooze, R. P., Eds.; Springer: Dordrecht, 2006. (d) Short, P. L. *Chem. Eng. News* **2006**, *84*, 15. (e) Keskin, S.; Kayrak, D.; Akman, U.; Hortacsu, O. *J. Supercrit. Fluids* **2007**, *43*, 150.

(11) Plechkova, N. V.; Seddon, K. R. *Chem. Soc. Rev.* **2008**, *37*, 123.

(12) (a) Dávila, M. J.; Aparicio, S.; Alcalde, R.; García, B.; Leal, J. M. *Green Chem.* **2007**, *9*, 221. (b) Aparicio, S.; Alcalde, R.; García, B.; Leal, J. M. *J. Phys. Chem. B* **2009**, *113*, 5593.

(13) Pernak, J.; Goc, I. *Pol. J. Chem.* **2003**, *77*, 975.

(14) Aparicio, S.; Alcalde, R. *Green Chem.* **2009**, *11*, 65.

(15) Latala, A.; Nedzi, M.; Stepnowski, P. *Green Chem.* **2009**, *11*, 1371.

(16) Pernak, J.; Goc, I.; Mirska, I. *Green Chem.* **2004**, *6*, 323.

(17) Petkovic, M.; Fergusson, J.; Bohn, A.; Trindade, J.; Martins, I.; Carvalho, M. B.; Leitao, M. C.; Rodrigues, C.; Garcia, H.; Ferreira, R.; Seddon, K. R.; Rebelo, L. P. N.; Silva, C. *Green Chem.* **2009**, *11*, 889.

(18) Padua, A. A. H.; Costa, M. F.; Canongia, J. N. A. *Acc. Chem. Res.* **2007**, *40*, 1087.

(19) (a) Burrell, A. K.; Del Sesto, R. E.; Baker, S. N.; McCleskey, M.; Baker, G. A. *Green Chem.* **2007**, *9*, 449. (b) Earle, M. J.; Gordon, C. M.; Plechkova, N. V.; Seddon, K. R.; Welton, T. *Anal. Chem.* **2007**, *79*, 758.

(20) Holbrey, J. D.; Seddon, K. R.; Wareing, R. *Green Chem.* **2001**, *3*, 33.

(21) Farmer, V.; Welton, T. *Green Chem.* **2002**, *4*, 97.

(22) Lemmon, E. W.; McLinden, M. O.; Friend, D. G. Thermophysical Properties of Fluid Systems. In *NIST Chemistry WebBook*; Linstrom, P. J., Mallard, W. G., Eds.; NIST Standard Reference Database Number 69; National Institute of Standards and Technology: Gaithersburg, MD, June 2005 (http://webbook.nist.gov).

(23) Viswanath, D. S.; Natarajan, G. *Data Book on the Viscosity of Liquids*; Hemisphere: New York, 1989.

(24) Cerdeiriña, C. A.; Migues, I. A.; Carballo, E.; Tovar, C. A.; de la Puente, E.; Romaní, L. *Thermochim. Acta* **2000**, *347*, 37.

(25) Zabransky, M.; Ruzicka, V.; Majer, V.; Domalski, E. Heat Capacities of Liquids. Critical Review and Recommended Values. *J. Phys. Chem. Ref. Data, Monogr.* **1996**, No. 6.

(26) Benson, G. C.; Kiyohara, O. *J. Chem. Thermodyn.* **1979**, *11*, 106.

(27) Douheret, G.; Moreau, C.; Viallard, A. *Fluid Phase Equilib.* **1985**, *22*, 277.

(28) García, B.; Aparicio, S.; Alcalde, R.; Ruiz, R.; Dávila, M. J.; Leal, J. M. *J. Phys. Chem. B* **2004**, *108*, 3024.

(29) Aparicio, S.; Alcalde, R.; García, B.; Leal, J. M. *Chem. Phys. Lett.* **2007**, *444*, 252.

(30) Frisch, M. J.; Trucks, G. W.; Schlegel, H. B.; Scuseria, G. E.; Robb, M. A.; Cheeseman, J. R.; Montgomery, J. A., Jr.; Vreven, T.; Kudin, K. N.; Burant, J. C.; Millam, J. M.; Iyengar, S. S.; Tomasi, J.; Barone, V.; Mennucci, B.; Cossi, M.; Scalmani, G.; Rega, N.; Petersson, G. A.; Nakatsuji, H.; Hada, M.; Ehara, M.; Toyota, K.; Fukuda, R.; Hasegawa, J.; Ishida, M.; Nakajima, T.; Honda, Y.; Kitao, O.; Nakai, H.; Klene, M.; Li, X.; Knox, J. E.; Hratchian, H. P.; Cross, J. B.; Adamo, C.; Jaramillo, J.; Gomperts, R.; Stratmann, R. E.; Yazyev, O.; Austin, A. J.; Cammi, R.; Pomelli, C.; Ochterski, J. W.; Ayala, P. Y.; Morokuma, K.; Voth, G. A.; Salvador, P.; Dannenberg, J. J.; Zakrzewski, V. G.; Dapprich, S.; Daniels, A. D.; Strain, M. C.; Farkas, O.; Malick, D. K.; Rabuck, A. D.; Raghavachari, K.; Foresman, J. B.; Ortiz, J. V.; Cui, Q.; Baboul, A. G.; Clifford, S.; Cioslowski, J.; Stefanov, B. B.; Liu, G.; Liashenko, A.; Piskorz, P.; Komaromi, I.; Martin, R. L.; Fox, D. J.; Keith, T.; Al-Laham, M. A.; Peng, C. Y.; Nanayakkara, A.; Challacombe, M.; Gill, P. M. W.; Johnson, B.; Chen, W.; Wong, M. W.; Gonzalez, C.; Pople, J. A. *Gaussian 03*, Revision C.02; Gaussian, Inc.: Wallingford, CT, 2004.

(31) Becke, A. D. *Phys. Rev. A* **1988**, *38*, 3098.

(32) Lee, C.; Yang, W.; Parr, R. G. *Phys. Rev. B* **1988**, *37*, 785.

(33) Becke, A. D. *J. Chem. Phys.* **1993**, *98*, 5648.

(34) Singh, U. C.; Kollman, P. A. *J. Comput. Chem.* **1984**, *5*, 129.

(35) Besler, B. H.; Merz, K. M.; Kollman, P. A. *J. Comput. Chem.* **1990**, *11*, 431.

(36) Simon, S.; Duran, M.; Dannenberg, J. J. *J. Chem. Phys.* **1996**, *105*, 11024.

(37) Ponder, J. W. *TINKER: Software tool for molecular design*, 4.2 ed.; Washington University School of Medicine: St. Louis, MO, 2004.

(38) Hoover, W. G. *Phys. Rev. A* **1985**, *31*, 1695.

(39) Allen, M. P.; Tildesley, D. J. *Computer Simulation of Liquids*; Clarendon Press: Oxford, U.K., 1989.

(40) Rickaert, J. P.; Ciccotti, G.; Berendsen, H. J. *J. Comput. Phys.* **1977**, *23*, 327.

(41) Essmann, U. L.; Perera, M. L.; Berkowitz, T.; Darden, H.; Lee, H.; Pedersen, L. G. *J. Chem. Phys.* **1995**, *103*, 8577.

(42) Martínez, J. M.; Martínez, L. *J. Comput. Chem.* **2003**, *24*, 819.

(43) Friedlander, A.; Martínez, J. M.; Santos, S. A. *Appl. Math. Opt.* **1994**, *30*, 235.

(44) Jorgensen, W. L.; Maxwell, D. S.; Tirado-Rives, J. *J. Am. Chem. Soc.* **1996**, *118*, 11225.

(45) Berendsen, H. J. C.; Grigera, J. R.; Straatsma, T. P. *J. Phys. Chem.* **1987**, *91*, 6269.

(46) Wakai, C.; Oleinikova, A.; Ott, M.; Weingärtner, H. *J. Phys. Chem. B* **2005**, *109*, 17028.

(47) Bright, F. V.; Baker, G. A. *J. Phys. Chem. B* **2006**, *110*, 5822.

(48) Köddermann, T.; Wertz, C.; Heintz, A.; Ludwig, R. *Angew. Chem., Int. Ed.* **2006**, *45*, 3697.

(49) Singh, T.; Kumar, A. *J. Phys. Chem. B* **2008**, *112*, 12968.

(50) Schrödle, S.; Annat, G.; MacFarlane, D. R.; Forsyth, M.; Buchner, R.; Hefter, G. *Chem. Commun.* **2006**, 1748.

(51) Weingärtner, H.; Padmanabhan, S.; Daguenet, C.; Dyson, P. J.; Krossing, I.; Slattery, J. M.; Schubert, T. *J. Phys. Chem. B* **2007**, *111*, 4775.

(52) Stoppa, A.; Hunger, J.; Buchner, R.; Hefter, G.; Thoman, A.; Helm, H. *J. Phys. Chem. B* **2008**, *112*, 4854.

(53) Aparicio, S.; Halajian, S.; Alcalde, R.; García, B.; Leal, J. M. *Chem. Phys. Lett.* **2008**, *454*, 49.

(54) Daguenet, C.; Dyson, P. J.; Krossing, I.; Oleinikova, A.; Slattery, J.; Wakai, C.; Weingärtner, H. *J. Phys. Chem. B* **2006**, *110*, 12682.

(55) Köddermann, T.; Heintz, A.; Wertz, C.; Ludwig, R. *ChemPhysChem* **2006**, *7*, 1944.

(56) Schröder, C.; Haberler, M.; Steinhauser, O. *J. Chem. Phys.* **2008**, *128*, 134501.

(57) Reichardt, C. *Green Chem.* **2005**, *7*, 339.

(58) Uusi-Penttilä, M. S.; Richards, R. J.; Torgerson, B. A.; Berglund, K. A. *Ind. Eng. Chem. Res.* **1997**, *36*, 510.

(59) Weingärtner, H. *Z. Phys. Chem.* **2006**, *220*, 1395.
(60) Hunger, J.; Stoppa, A.; Buchner, R.; Hefter, G. *J. Phys. Chem. B* **2009**, *129*, 9527.
(61) Seddon, K. R.; Stark, A.; Torres, M. J. *Pure Appl. Chem.* **2000**, *72*, 2275.
(62) Cammarata, L.; Kazarian, S. G.; Salter, P. A.; Welton, T. *Phys. Chem. Chem. Phys.* **2001**, *3*, 5192.
(63) Averett, L. A.; Griffiths, P. R.; Noshikida, K. *Anal. Chem.* **2008**, *80*, 3045.
(64) Tran, C.; De Paoli, S.; Oliveira, D. *Appl. Spectrosc.* **2003**, *57*, 152.
(65) Cuadrado, S.; Dominguez, M.; García, S.; Segade, L.; Franjo, C.; Cabeza, O. *Fluid Phase Equilib.* **2009**, *278*, 36.
(66) van Valkenburg, M. E.; Vaughn, R. L.; Williams, M.; Wilkes, J. S. *Thermochim. Acta* **2005**, *425*, 181.
(67) *NIST Ionic Liquids Database, ILThermo*; NIST Standard Reference Database 147; National Institute of Standards and Technology Standard Reference Data Program: Gaithersburg, MD, 2006. http://ILThermo.boulder.nist.gov/ILThermo/.
(68) Xu, W.; Cooper, E. I.; Angell, C. A. *J. Phys. Chem. B* **2003**, *107*, 6170.
(69) Zhang, Z. Z.; Chang, Z.; Xu, K.; Angell, C. A. *Electrochim. Acta* **2000**, *45*, 1229.
(70) Anouti, M.; Caillon, M.; Le Floch, C.; Lemordant, D. *J. Phys. Chem. B* **2008**, *112*, 9412.
(71) Angell, C. A. *Science* **1995**, *267*, 1924.
(72) MacFarlane, D. R.; Forsyth, M.; Izgorodina, E. I.; Abbott, A. P.; Annat, G.; Fraser, K. *Phys. Chem. Chem. Phys.* **2009**, *11*, 4962.
(73) Zhao, C.; Burrell, G.; Torriero, A. A. J.; Separovis, F.; Dunlop, N. F.; MacFarlane, D. R.; Bond, A. M. *J. Phys. Chem. B* **2008**, *112*, 6923.
(74) Fraser, K. J.; Izgorodina, E. I.; Forsyth, M.; Scott, J. L.; MacFarlane, D. R. *Chem. Commun.* **2007**, 3817.
(75) (a) Shah, J. K.; Brennecke, J. F.; Maginn, E. J. *Green Chem.* **2002**, *4*, 112. (b) Shah, K. K.; Maginn, E. J. *Fluid Phase Equilib.* **2004**, *222*−*223*, 195. (c) Cadena, C.; Zhao, Q.; Snurr, R.; Maginn, E. J. *J. Phys. Chem. B* **2006**, *110*, 2821. (d) Bhargava, B. L.; Balasubramanina, S. *J. Chem. Phys.* **2007**, *127*, 114510. (e) Liu, X.; Zhou, G.; Zhang, S. *Fluid Phase Equilib.* **2008**, *272*, 1.
(76) Liu, X.; Zhang, S.; Zhou, G.; Wu, G.; Yuan, X.; Yao, X. *J. Phys. Chem. B* **2006**, *110*, 12062.
(77) Canongia, J. N. A.; Padua, A. H. *J. Phys. Chem. B* **2006**, *110*, 3330.
(78) Köddermann, T.; Paschek, D.; Ludwig, R. *ChemPhysChem* **2008**, *9*, 549.
(79) Armstrong, J. P.; Hunt, C.; Jones, R. G.; Licence, P.; Lovelock, K. R. J.; Satterley, C. J.; Villar-García, I. J. *Phys. Chem. Chem. Phys.* **2007**, *9*, 982.
(80) Dupont, J. *J. Braz. Chem. Soc.* **2004**, *15*, 341.
(81) Hunger, J.; Stoppa, A.; Buchner, R.; Hefter, G. *J. Phys. Chem. B* **2008**, *112*, 12913.
(82) Buchner, R.; Barthel, J.; Stauber, J. *Chem. Phys. Lett.* **1999**, *306*, 57.
(83) Jarosik, A.; Krajewski, S. R.; Lewandowski, A.; Radzimski, P. *J. Mol. Liq.* **2006**, *123*, 43.
(84) Harifi-Mood, A. R.; Habibi-Yangjeh, A.; Gholami, M. R. *J. Phys. Chem. B* **2006**, *110*, 7073.
(85) Brooksby, P. A.; Fawcett, R. *J. Phys. Chem. A* **2000**, *104*, 8307.
(86) Jeon, Y.; Sung, J.; Kim, D.; Seo, C.; Cheong, H.; Ozawa, R.; Hamaguchi, H. *J. Phys. Chem. B* **2008**, *112*, 923.
(87) Liu, D.; Ma, G.; Levering, L. M.; Allen, H. C. *J. Phys. Chem. B* **2004**, *108*, 2252.
(88) Rodríguez, H.; Brennecke, J. F. *J. Chem. Eng. Data* **2006**, *51*, 2145.
(89) Khupse, N. D.; Kumar, A. *J. Sol. Chem.* **2009**, *38*, 589.
(90) Aparicio, S.; Alcalde, R. *J. Phys. Chem. B* **2009**, *113*, 14257.
(91) Jiang, W.; Wang, Y.; Voth, G. A. *J. Phys. Chem. B* **2007**, *111*, 4812.

JP911536Z